HHS Public Access

Author manuscript

Biochemistry. Author manuscript; available in PMC 2016 August 04.

Published in final edited form as:

Biochemistry. 2015 August 4; 54(30): 4652–4664. doi:10.1021/acs.biochem.5b00573.

Rate-determining Attack on Substrate Precedes Rieske Cluster Oxidation during *cis*-Dihydroxylation by Benzoate Dioxygenase

Brent S. Rivard[†], **Melanie S. Rogers**[†], **Daniel J. Marell**[‡], **Matthew B. Neibergall**[†], **Sarmistha Chakrabarty**[†], **Christopher J. Cramer**[‡], and **John D. Lipscomb**[*,†]

[†]Department of Biochemistry, Molecular Biology, and Biophysics and the Center for Metals in Biocatalysis, University of Minnesota, Minneapolis, Minnesota 55455

[‡]Department of Chemistry, Chemical Theory Center, and Supercomputing Institute, University of Minnesota, Minneapolis, Minnesota 55455

Abstract

Rieske dearomatizing dioxygenases utilize a Rieske iron-sulfur cluster and a mononuclear Fe(II) located 15 Å across a subunit boundary to catalyze O_2-dependent formation of *cis*-dihydrodiol products from aromatic substrates. During catalysis, O_2 binds to the Fe(II) while the substrate bind nearby. Single turnover reactions have shown that one electron from each metal center is required for catalysis. This finding suggested that the reactive intermediate is Fe(III)-(H)peroxo or HO-Fe(V)=O formed by O-O bond scission. Surprisingly, several kinetic phases were observed during the single turnover Rieske cluster oxidation. Here, the Rieske cluster oxidation and product formation steps of a single turnover of benzoate 1,2-dioxygenase are investigated using benzoate and three fluorinated analogs. It is shown that the rate constant for product formation correlates with the reciprocal relaxation time of only the fastest kinetic phase (RRT-1) for each substrate, suggesting that the slower phases are not mechanistically relevant. RRT-1 is strongly dependent on substrate type, suggesting a role for substrate in electron transfer from the Rieske cluster to the mononuclear iron site. This insight, together with the substrate and O_2 concentration dependencies of RRT-1, indicates that a reactive species is formed after substrate and O_2 binding, but before electron transfer from the Rieske cluster. Computational studies show that RRT-1 is correlated

[*]**Corresponding author** Address: (J.D.L.) Department of Biochemistry, Molecular Biology, and Biophysics, 6-155 Jackson Hall, University of Minnesota, 321 Church St. SE, Minneapolis, MN 55455; Telephone, (612) 625-6454; fax, (612) 624-5121; Lipsc001@umn.edu.

[a]In most characterized RDDs, the as-isolated state of the enzyme is composed of 100% oxidized Rieske cluster (Fe(III)Fe(III)) and 100% ferrous mononuclear Fe.[7] No equilibrium is observed between the reduced mononuclear Fe and the oxidized Rieske cluster showing that the reduction potentials are far enough apart that the electron transfer is irreversible. BZDO is unique in that it can be isolated in either the typical state or in a fully oxidized state with a ferric mononuclear Fe.[52] When BZDO is fully oxidized, addition of stoichiometric reducing equivalents (relative to active sites) from dithionite results in the typical state of oxidized Rieske cluster and ferrous mononuclear Fe.[52] The reduction potentials of the Rieske cluster and mononuclear Fe for the Rieske monooxygenase putidamonoxin have been reported as 5 mV and ≥ 200 mV respectively.[53,54]

[b]The good correlation illustrated in Figure 6 is independent of whether the C(2)–H charges are computed for the conjugate acid (proximally or distally oriented) or base forms of the benzoates (R^2 values of 0.992 or higher), but the correlation *is* sensitive to whether the charges are computed in the gas phase or including solvation effects. The correlation is significantly improved when using solvated values, as might be expected given the condensed-phase nature of the reaction.

The authors declare no competing financial interests.

ASSOCIATED CONTENT

Supporting experimental procedures, results, Figures S1–S3. This material is available free of charge via the Internet at http://pubs.acs.org.

with the electron density at the substrate carbon closest to the Fe(II), consistent with initial electrophilic attack by an Fe(III)-superoxo intermediate. The resulting Fe(III)-peroxo-aryl radical species would then readily accept an electron from the Rieske cluster to complete the *cis*-dihydroxylation reaction.

Rieske oxygenases catalyze a diverse repertoire of chemical reactions including oxygenation of hydrocarbons, O- and N-demethylations, N-oxidations, and C-C bond formation in pathways for catabolism of hydrocarbons, and biosynthesis of medically significant natural products.[1] The Rieske oxygenase subclass termed Rieske dearomatizing dioxygenases (RDDs) are the only known enzymes that catalyze dearomatizing *cis*-dihydroxylation of aromatic compounds (Scheme 1). This reaction activates otherwise stable aromatic compounds, making RDDs effective agents for bioremediation.[2, 3] Another type of application stems from the ability of RDDs to produce large quantities of regio and stereospecific *cis*-diols as important synthetic building blocks for streamlining synthesis of drugs and antibiotics.[4] A complete understanding of the catalytic mechanism of RDDs will aid further development and utilization of these applications and provide guiding insights for mechanistic studies of the broad class of Rieske oxygenases.

The benzoate 1,2-dioxygenase system is an archetypal RDD that utilizes the electrons from NADH to catalyze the conversion of benzoate to (1S,6R)-1,6-*cis*-dihydroxycyclohexa-2,4-diene-1-carboxy acid (benzoate *cis*-diol), inserting both atoms from O_2 into the substrate, forming the product (Scheme 1).[5–7] This system consists of reductase (BZDR) and oxygenase (BZDO) components. Each α-subunit of the $(\alpha\beta)_3$ BZDO contains a [2Fe-2S] Rieske cluster and a nonheme mononuclear Fe coordinated by two His and one Asp residues (a 2-His-1-carboxylate facial triad)[8] in addition to 1 or 2 solvent molecules.[9, 10] The conserved quaternary structure of RDDs places the Rieske cluster of one α-subunit within 15 Å of the mononuclear iron of the adjacent α-subunit, suggesting that this pair of metal centers comprise the functional unit of the enzyme.[10, 11] Substrates bind near (but not to) the mononuclear Fe, showing that this is the site of O_2 activation and *cis*-dihydroxylation.[12–15] Single turnover experiments have shown that reduction of both the Rieske cluster and the mononuclear iron is required for normal catalysis, and that one electron from each metal center is used during the *cis*-dihydroxylation reaction.[7] A conserved Asp residue links the two metal centers via hydrogen bonding and appears to mediate the electron transfer from the Rieske cluster to the mononuclear iron during the reaction. [11, 16, 1718, 19] Conformational changes involving the pathway between the metal centers also appear to play a role in the complex regulatory mechanism of the enzyme, which ensures that the Rieske cluster is reduced and substrate is correctly bound in the active site before O_2 can be activated at the mononuclear Fe(II). [9, 20–22] This mitigates formation of deleterious reactive oxygen species.[7, 23]

RDDs have characteristics that make them mechanistically distinct from other Fe-dependent dioxygenases and monooxygenases. For example, many non-heme dioxygenase classes that are reactive in the Fe(II) state utilize the 2-His-1-carboxylate facial triad iron binding ligation like the RDDs. [24] However, these dioxygenases extract all four electrons required for O_2 reduction from the substrate or co-substrate, whereas RDDs ultimately utilize two

electrons from the substrate and two from NADH. Monooxygenases like methane monooxygenase (MMO) or cytochrome P450, also extract two electrons from both substrate and NADH, but the products are oxidized substrate and water rather than a dihydroxylated substrate. [25–27] It is noteworthy that well-characterized Rieske monooxygenases exists which are structurally similar to RDDs, but exhibit the same NADH and O_2 stoichiometry and single oxygen atom incorporation pattern as MMO or cytochrome P450.[20, 28] These similarities have led mechanistic theories for RDDs along the lines of monooxygenase rather than dioxygenase enzymes.

A hypothesis for the mechanism of RDDs based on typical monooxygenase chemistry is shown in Scheme 2 (purple arrows).[7] Substrate binds to the enzyme with the Rieske cluster and mononuclear Fe reduced ($Rieske^{red}$ / Fe(II)), resulting in solvent release from the mononuclear Fe(II). Then, O_2 binds to the Fe(II) and an electron from the reduced Rieske cluster is transferred to the mononuclear Fe-O_2 complex to yield a (hydro)peroxo intermediate similar to those previously proposed for all well-characterized monooxygenases.[29–33] The (hydro)peroxo species might be reactive with substrate or the O-O bond could cleave to yield a reactive HO-Fe(V)=O species (red bracketed box in Scheme 2).

The results from experimental and computational approaches have supported the monooxygenase-like mechanism of RDD catalysis, but have not agreed on the identity of the reactive species performing the initial substrate oxidation.[1, 24] *In crystallo* characterization of tertiary ESO_2 complexes in the RDDs naphthalene 1,2-dioxygenase (NDO) and carbazole 1,9a–dioxygenase (CarDO) have shown O_2 binding in side-on or end-on configuration to the mononuclear iron, resulting in lengthening of the O-O bond consistent with formation of a peroxo species.[13, 15] Also, BZDO with both the mononuclear Fe and Rieske cluster oxidized can form significant yields of product after addition of substrate and H_2O_2 in a peroxide shunt reaction (Scheme 2, blue arrows).[34] During these reactions, the observed rate constants of single turnover is decreased by a factor of ~ 2×10^5. Analysis of the peroxide shunt reaction revealed formation of a transient $S = 5/2$ ferric species with unusual spectroscopic properties consistent with those of a side-on bound Fe(III)-(hydro)peroxo species. These observations suggest that an Fe(III)-(hydro)peroxo is on the reaction coordinate during peroxide shunt reactions and may also be important during catalytic turnover.

DFT studies based on active site models of the structurally homologous RDDs NDO and nitrobenzene 1,2-dioxygenase (NBDO) have reached different conclusions regarding the reaction coordinate. The calculations with NDO showed that O-O bond cleavage prior to substrate attack to yield an HO-Fe(V)=O is too energetically demanding. Instead, a lower energy pathway was proposed using a side-on Fe(III)-(hydro)peroxo proceeding to product through an epoxide intermediate.[35] However, recently conflicting results were obtained in a study of NBDO which showed that such a peroxo attack is more energetic than O-O bond cleavage. [36]

Several insights have been gained from studies with small-molecule Fe-chelate complexes that mimic the active site of RDDs. Investigations of olefin oxidation using various

complexes showed two distinct reactive pathways to *cis*-dihydroxylation.[37] Both types of reaction rely on the availability of two adjacent ligand sites on the iron, as is apparently the case for RRDs. In one type of reaction catalyzed by some low spin Fe(III)-(hydro)peroxo complexes within TPA or BPMEN ligands, one oxygen from water is incorporated into the *cis*-diol product in addition to one oxygen from H_2O_2. [38] This observation and subsequent experiments have demonstrated a water assisted cleavage of the O-O bond to form an HO-Fe(V)=O reactive species. [39] In contrast, both *cis*-diol oxygens were found to derive from peroxide when the reactions were carried out with high-spin TPA and BPMEN Fe-chelate compounds.[37] The mononuclear iron of RDDs is high spin in both the ferric and ferrous state,[7] but whether this correlates with the type of reactive species formed is unknown. Another study using high-spin TMC-Fe(III)-hydroperoxo complexes has shown that the S = 5/2 state increased the oxidation potential. [40] This generates a more potent species for electrophilic catalysis, thereby providing evidence that an Fe-hydroperoxo could be active in RDDs.

The focus on two-electron O_2 activation in RDDs has limited consideration of another commonly employed mechanistic strategy in the 2-His-1-carboxylate family involving one electron reduced O_2. Indeed, the initial attacking species in enzymes such as extradiol ring-cleaving dioxygenases[41, 42] and isopenicillin N-synthase [43] are proposed to be metal-bound superoxo moieties.[44, 45]

A potential difficulty with a mechanism that invokes an Fe(III)-peroxo or HO-Fe(V)=O, reactive species for RDDs derives from our past studies which showed that the rate of electron transfer from the Rieske cluster to the mononuclear iron site within BZDO is influenced by the functional groups on the aromatic ring of benzoate.[7] This observation might imply that the reaction of some type of Fe-oxygen intermediate with substrate occurs before formation of a two-electron reduced species. Alternatively, it could reflect steric effects on the substrate position in the active site. Here, the transient kinetics of electron transfer within BZDO during a single turnover are examined for benzoate and a variety of fluorinated benzoates selected in order to limit steric effects. It is shown that the step in which activated O_2 first attacks the substrate is rate limiting, and that this step is likely to involve a metal-bound species with superoxo character. The study provides new insight into the detailed steps of oxygen activation and reaction that ensure both specificity and efficient catalysis in Rieske dioxygenases.

EXPERIMENTAL PROCEDURES

Standard materials and procedures are described in Supporting Information. Authentic standards of dearomatized 1,2-*cis*-diol products of benzoate and the fluorobenzoates used here were prepared and characterized as described in Supporting Information. Cloning, heterologous expression, and purification of BZDO and BZDR from the genomic DNA of *Pseudomonas putida* mt-2 were carried out using modifications of previously described methods.[7] The current methods for these procedures are described in Supporting Information.

Stopped-Flow Analysis of Single Turnover Reactions

Stopped-flow experiments were performed at 4 °C, in 50 mM MOPS buffer, pH 6.8 plus 100 mM NaCl using an Applied Photophysics SX.18MV configured for single wavelength data collection at 464 nm. The instrument was made anaerobic by flushing with a dithionite solution and then anaerobic buffer. BZDO (60 μM) was reduced as described in the Supporting Information and mixed with a solution containing varied concentrations of substrate and O_2 (see figure legends). Fitting procedures for time courses to multiexponential equations and concentrations dependencies to hyperbolic expressions are described in Supporting Information.

Chemical Quench and Rapid Chemical Quench Product Analysis

Reduced BZDO (400 μM) was mixed 1:1 with reaction buffer (50 mM MOPS buffer, pH 6.8 plus 100 mM NaCl) saturated with O_2 (1.8 mM at 4 °C) containing benzoate or a fluorobenzoate (10 mM). For time point quenches of completed reactions (> 3 min), 200 μl of the reaction mixture was pipetted into 800 μl of rapidly stirring 1 M HCl. Rapid quenches were accomplished in an identical manner except that an Update 715 ram Syringe Controller was used to mix and dispense the reactants. Sodium formate (50 μl of 7.5 M) and NaOH (50 μl of 10 M) were added to the quenched solution to buffer the pH to ≈ 3.5 and 400 μl H_2O was added to bring the final volume up to 1.5 ml. Each sample was vortexed (~20 s) and the denatured protein was removed from the solution by centrifugation at 4 °C before HPLC was used to analyze 1 ml of the quenched reaction. HPLC was performed on a Waters system with a 1525 binary pump, 2487 dual wavelength UV/Vis detector, and an Agilent Zorbax SB C18 column (4.6 mm × 150 mm, 5 μm) with an aqueous gradient of 4 to 100% acetonitrile/0.1% formic acid over 7.5 min following an isocratic flow at 4% acetonitrile/ 0.1% formic acid for 2.5 min. The *cis*-diol products were detected by their optical absorption at 262 nm. The methods used to verify the observed HPLC peaks and construct standard curves for quantification using authentic standards are described in the Supporting Information.

Computational methods

Molecular geometries for parent and various fluoro-substituted benzoic acids were optimized at the M06-2X level of density functional theory[46] employing the 6–311+(2df,p) basis set.[47] Both conjugate acid and conjugate base forms were considered in the optimizations, and the calculations were undertaken both in the gas phase and also including condensed phase effects using the SMD continuum aqueous solvation model.[48, 49] Charges were computed for the optimized structures at the same level of theory employed for the optimizations, summing the charges for carbon atoms with those for attached H atoms in order to compute a net group partial charge for the C(2) C–H group. In the case of the conjugate acids, variations in this charge as a function of the position of the hydroxyl group of the carboxylic acid (distal or proximal to the carbon defined as C(2)) was in every instance 0.009 a.u. for gas-phase calculations, but no more than 0.001 a.u. with the SMD solvation model. Geometry optimizations were accomplished with the Gaussian09 suite of electronic structure programs[50] and CM5 charges were computed using CM5PAC.[51]

RESULTS

Product Formation Correlates with Only One Step of the Multistep Rieske Cluster Oxidation Reaction

Single turnover reactions were conducted by rapidly mixing reduced BZDO in a stopped-flow instrument with buffer containing substrate and O_2 (saturated). Only a single turnover can occur because there is no additional reductant present to reduce the metal centers for a second turnover, and the ferric mononuclear iron must be reduced in order for product to dissociate.[7] Figure 1 shows that spectra collected during single turnover reactions monitored in this study fit well as linear combinations of the fully oxidized and reduced Rieske cluster spectra, demonstrating that no other chromophoric intermediate(s) accumulate to detectable concentrations.

Figure 2A shows the single wavelength time courses of Rieske cluster oxidation during single turnover reactions containing benzoate or one of several fluorinated benzoates selected to yield only one *cis*-diol product. Each reaction displayed two characteristics previously observed for the turnover of other substrates.[7] First, a satisfactory simulation of the time course of the Rieske cluster oxidation under pseudo-first order conditions requires more than one exponential phase term (Figure 2B). This shows that there is more than one step in the Rieske cluster oxidation process for each substrate, but it does not indicate whether the steps occur in sequence or in parallel, or whether all of the steps are catalytically relevant. Second, the chemical nature of the substrate (in this case, the number and position of the fluorine aromatic substituents) changes the magnitudes of observed reciprocal relaxation times (RRTs). (Figure 2A and Table 1).

The catalytic relevance of the steps in a multistep reaction can sometimes be evaluated from the magnitudes of the RRTs in comparison to the k_{cat} values for the reactions. This is straight forward when the steps are irreversible, in which case each RRT is the rate constant for a specific step. Many of the steps in the current case are likely to be effectively irreversible: electron transfer across a substantial potential gradient.[a, 52–54] O-O bond cleavage, and *cis*-dihydroxylation. (The conclusion of irreversible steps is verified by results shown below.) With benzoate as the substrate, three substrate-dependent (see below) exponential phases are observed, while the reactions for the fluorobenzoates each exhibit only two substrate-dependent phases. All the substrate-dependent phases are faster than the respective k_{cat} values for the reactions, and thus all of the corresponding steps (assumed to be irreversible) must initially be considered relevant to the true catalytic process of the enzyme (Table 1). In contrast, each reaction displayed one or more low amplitude substrate concentration independent phases with RRTs much slower than k_{cat} and are therefore not catalytically relevant. Despite the observation of at least two kinetically relevant phases, it is difficult to rationalize how a single, one electron, Rieske cluster oxidation event could occur in a multistep sequential reaction. Thus, it is important to identify functionally relevant steps, which may be a subset of kinetically competent steps.

One strategy that may distinguish functionally relevant from nonproductive Rieske oxidation steps is to determine the number of steps involved in product formation and their rate constant(s). Rapid chemical-quench samples taken at specific times during a single

turnover were analyzed by HPLC to determine the rate constant(s) and fractional yield of product formation as shown in Figure 3 and S1 and summarized in Table 1. For each substrate, a single new HPLC peak appears at the same retention time as purified authentic standards of the *cis*-diol product (Figures 3 and S1, insets). In contrast to the time course for Rieske cluster oxidation, the accumulation of *cis*-diol products can be fit to a single exponential function (Figures 3 and S1). For each substrate, the k_{obs} for product formation is within experimental error of RRT-1 (Table 1). Under the assumption of irreversible steps in the product formation process, this suggests that the product is formed in only one step of the Rieske oxidation reaction. If so, then the fraction of the overall amplitude of the Rieske oxidation represented in RRT-1 should correlate with the fractional yield of each *cis*-diol product. It is shown in Table 1 that this prediction is confirmed. While the error in the yield data would allow additional phases in the fit, the small amount of product formed during these phases would not correlate with the amplitudes of the slower phases in the optically monitored time course. These results strongly imply that the observed phases do not arise from a multistep, sequential process, but instead are the result of independent, parallel, substrate-triggered Rieske oxidation reactions. The reason that the slower substrate-dependent steps do not yield product remains unclear. However, the ability to consider the catalytically relevant Rieske oxidation as a one-step process greatly simplifies the analysis of the mechanism of the *cis*-diol forming reaction. Accordingly, we will only consider RRT-1 here, and the RRT for this phase will be considered the rate constant for the rate-determining step in the product-forming process.

It is important to note that even though it is Rieske oxidation being monitored in the single step product forming reaction, the electron transfer *per se* between the Rieske cluster and mononuclear iron site is unlikely to be rate-limiting. In all of the structurally characterized RDDs, the electron transfer between the Rieske cluster and mononuclear iron occurs over a distance of about 15 Å presumably following a through-bond pathway[10, 11] with a large driving force due to the difference in redox potentials of the metal sites.[53, 54] A rate constant for electron transfer (k_{et} in Scheme 2) of 2.2×10^6 s^{-1} was computed based on the NDO active site structure.[55] This rate constant is four orders of magnitude larger than those for single turnover with benzoate, the fastest substrate in this study, thus, a step(s) that precedes the electron transfer must be rate-limiting. Nevertheless, the Rieske cluster oxidation allows the rate-determining step in product formation to be characterized and its rate constant determined, as shown below.

The Rate-Limiting Step Prior to Rieske Cluster Oxidation Occurs after Initial Substrate and O_2 Binding

One possible explanation for the large difference in rate of single turnover between benzoate and the fluorobenzoates is that the fluorine substituent(s) interferes with substrate and /or O_2 binding despite the comparable van der Waals radii of hydrogen and fluorine. This possibility was examined by studying the substrate and O_2 binding kinetics of each reaction through monitoring the Rieske cluster oxidation time course under pseudo-first order conditions in substrate and O_2. The rate constant for each substrate reaction exhibits a hyperbolic concentration dependence as shown in Figure 4A and S2A. This result shows that the oxidation of the Rieske cluster is not rate limited by substrate binding, and that the

binding reaction is reversibly connected to the true rate-limiting step. For this type of kinetic behavior (see Experimental Procedures in Supporting Information), the apparent K_d for the relatively fast (unobserved) binding reaction is given by the K_d for the titration curve. In the present case, the apparent K_d values for benzoate and 4-FB are approximately the same (Table 2). This result shows that replacing hydrogen with a fluorine substituent at carbon 4 does not affect binding affinity. The extrapolated y-intercept and the asymptotic maximum of the curve give information about the true rate-limiting step. In this case, the y-intercept for the titration plots is approximately zero, suggesting that the rate-limiting reaction in effectively irreversible, supporting the assumptions of irreversibility proposed above. The extrapolated maxima of the titration plots at high substrate concentration are quite different (Table 2), reflective of the substrate type-dependence of the true rate-limiting step.

The 3,5-fluorobenzoate and 3,4,5-fluorobenzoate substrates also exhibit hyperbolic concentration dependence extrapolating to zero (Figure S2A). Once again the maximum value for RRT-1 depends on the type of substrate present (Table 2). However, the apparent K_d values for the unobserved substrate binding step are an order of magnitude higher than those observed for benzoate and 4-fluorobenzoate. Apparently, the presence of fluorine at the 3 and/or 5 positions weakens the binding slightly without causing a change in the product formed. This pair of substrates shows similar values for the apparent K_d, as observed for the benzoate, 4-fluorobenzoate pair (Table 2).

Earlier studies have shown that O_2 binding requires both reduction of the Rieske cluster and prior substrate binding (Scheme 2). [7, 52] As shown in Figure 4B, the rate constant for the catalytically relevant step preceding Rieske cluster oxidation reaction displays a hyperbolic dependence under pseudo-first order conditions in O_2 and a large excess of benzoate or 4-FB over the apparent K_d values determined from Figure 4A. As described above for substrate binding, the hyperbolic plot shows that the O_2 binding reaction is not rate-limiting. The hyperbolic fits with zero y-intercepts and the similar apparent K_d values for the two substrates confirm that the true rate-limiting reaction is effectively irreversible and that the presence of a fluorine substituent(s) does not significantly affect O_2 binding affinity. The maxima ($k_{forward}$) of the fitted O_2 titration plots are different from each other, but similar to the respective values found for the substrate titration plots (Table 2). This suggests that the true rate-limiting step is substrate-type dependent, and that the rate constant for substrate and O_2 binding reactions are limited by the same downstream reaction. The same conclusions are reached for the O_2 binding reactions in the presence of 3,5-FB and 3,4,5-FB as shown in Figure S2B. In the case of O_2 binding, the substrate type causes little change in the apparent K_d.

Binding of the O_2 Surrogate Nitric Oxide to the Mononuclear Fe(II) is Fast Relative to the Rate of Product Formation

Studies of other oxygenases have indicated that O_2 binding might proceed in several steps beginning with the formation of a complex in the active site but not yet with the metal.[56–58] Indeed, a small molecule binding site has been identified in the active site of NDO.[59] As such, binding of O_2 to the mononuclear iron from an active site binding location might be rate-limiting. One means to directly observe small molecule binding to the metal utilizes NO

as an O_2 surrogate. [7, 60] The chemical and spatial environments of the resulting spin-coupled Fe(III)-NO^- complex can be probed via its characteristic S = 3/2 EPR spectrum and broad optical spectrum.[61, 62] The optical spectra of reduced BZDO exposed to NO (~ 0.5 equivalents relative to active sites) with and without added benzoate or 4-FB are shown in Figure 5A. In the absence of substrate, there is a large change in the intensity and shape of the optical absorption spectrum across the visible region, but a much smaller change in intensity and little change in spectral lineshape occurs in the presence of either substrate. The cause of this difference is revealed in EPR spectra (Figure 5A, inset) of identical samples. When NO was added to the reduced enzyme in the absence of substrate, the rhombic S = ½ EPR spectrum of the reduced Rieske cluster (g-values 2.01, 1.91, and 1.76)[7] was attenuated and a new species formed with spectral characteristics (g = 2.04) consistent with dinitrosyl iron complexes previously reported from reactions of biological Rieske clusters with NO.[63] When 4-FB was present, the predicted S =3/2 spectrum of a mononuclear Fe(III)-NO^- adduct appears without alteration of intensity or lineshape of the reduced Rieske cluster signal (Figure 5A, inset). This demonstrates that when substrate is present, NO binds preferentially to the mononuclear iron site, causing a broad increase in absorbance without significant change in the spectral line shape of the intense chromophore of the Rieske cluster.

The optical changes observed upon binding of sub-stoichiometric NO exclusively to the mononuclear Fe site in the presence of benzoate or 4-FB provides, in principle, a method to measure the rate constants for the binding reaction of NO, and by analogy O_2, to the metal. When sub-stoichiometric NO was rapidly mixed with solutions of reduced BZDO and benzoate or 4-FB (Figure 5B), the change in absorbance occurred primarily in the dead time of the stopped-flow instrument (pseudo-first order rate constant ≥ 600 s^{-1}). These results show that NO, and presumably O_2, in the presence of substrates bind with a much larger pseudo-first order rate constant than the rate constant for the true rate-limiting step prior to the Rieske oxidation reaction.

The Rate Constant for the Rate-Limiting Step Correlates with the Computed Atomic Charge at the Site of Attack on Substrate

An alternative explanation for the difference in single turnover rates of benzoate and the fluorobenzoates is that the electronegative fluorine aromatic substituents deactivate the substrates with respect to electrophilic attack on the aromatic ring. If this hypothesis is true, a relationship should exist that correlates the electronic changes within the fluorobenzoates listed in Table 1 with the rate constants for Rieske cluster oxidation. As shown in Figure S3, this system is not described well by a Hammett σ plot. However, Hammett analysis is more typically successful for reactions occurring at benzylic positions than at aromatic ring centers themselves. A more direct approach to this analysis was adopted by calculating the partial atomic charge specifically at carbons 1 (the ipso carbon) and 2 for benzoate and the fluorobenzoates and then comparing this value to RRT-1 under saturating conditions for each substrate. While there is no trend associated with the CM5 partial charge for carbon 1 (nor is any trend apparent when correlating rates against computed frontier orbital energies), a linear relationship was observed between the observed rates and the CM5 partial group charge at carbon 2 (Figure 6) indicating that as electron density is removed from carbon 2,

the rate of electron transfer from the Rieske cluster decreases proportionally.[b] The suggestion that the C(2)–H group is the site of initial reaction is supported by structural studies of NBDO, which is similar to BZDO in structure, substrate, and chemistry.[14] In NBDO, substrate carbon 2 is positioned closer to the mononuclear Fe than carbon 1, and is thus the likely site of initial attack of the activated oxygen species. This result is consistent with the hypothesis that the decreased rate of turnover with the fluorobenzoates is caused by a change in electron density at the site of initial substrate oxidation.

DISCUSSION

The results presented here show that the rate-determining step of product formation in the active site of BZDO occurs after substrate and O_2 binding, but before transfer of an electron from the Rieske cluster to the mononuclear iron site. This finding contradicts all previous mechanistic theory for RDDs. [7, 52, 55, 64, 65] In these earlier studies, it was proposed that the reactive species is an Fe(III)-(H)peroxo adduct (or the derivative HO-Fe(V)=O), which requires transfer of a Rieske electron prior to its formation. Our finding implies a new reactive species for RDDs and differentiates the potential mechanism from those proposed for other NAD(P)H-linked oxygenases such as cytochrome P450 and MMO.[27, 29, 66–68] These aspects of RDD catalysis are discussed here.

Significance of Product Forming in Only One Step of the Rieske Cluster Oxidation Process

A long standing mystery in the study of BZDO is the cause of the multiphase Rieske cluster oxidation observed during single turnover.[7] This phenomenon has also been reported for other RDDs such as phthalate and anthranilate dioxygenases. [17, 69] Several hypotheses were proposed in these studies to account for the multiphase oxidation including (anti)cooperativity between the subunits of the enzymes, asymmetry caused by partially occupied metal sites, and multistep sequential reactions. The finding here that only the RRT and amplitude of the fastest phase correlate with the rate constant and overall yield of product formation during a single turnover argues against multistep sequential reactions and subunit cooperativity. Rather, the data strongly imply that the Rieske cluster can oxidize in multiple, independent, one-step processes, only one of which is relevant to product formation. It is this insight that allows the evaluation of the steps in substrate binding, oxygen activation, and product formation described here.

Despite the observation that product is formed in only one of two or more independent Rieske oxidation reactions, it is true that the rate constants for some of the non-product forming reactions depend on both the type and concentration of substrate present. This implies substrate participation in each process, and consequently, a role for the mononuclear iron center where the substrate binds. The most straight forward explanation for this observation is that in each reaction an Fe-oxy species of some sort interacts with substrate to trigger the inter-subunit electron transfer. For the slower non-product forming processes, the reaction apparently does not carry through to *cis*-diol formation. Indeed, after a single turnover of BZDO, all of the Rieske cluster and mononuclear iron is oxidized despite the less than stoichiometric product yield.[7] This finding may be associated with release of H_2O_2 or another reduced oxygen species, as has been previously reported for some RDD

systems. [70–72] We have previously shown that BZDO can act as an effective catalase.[34, 64] Consequently, direct observation of H_2O_2 release during the non-product forming oxidation reactions of BZDO has not been verified.

Nature of the Reactive Species

The most plausible initial activated oxygen species after formation of an Fe(II)-O_2 complex is an Fe(III)-superoxo (Fe(III)-$O_2^{\bullet-}$) complex. Regulation in BZDO and the RDD family prevents such a complex from forming in the absence of substrate and a reduced Rieske cluster.[7, 52] This regulation appears to have at least two aspects. First, spectroscopic studies suggest that substrate binding may facilitate release of solvent blocking the potential O_2 binding site.[9] Second, spectroscopic and crystallographic studies suggest that reduction of the Rieske cluster may shift the mononuclear iron slightly relative to substrate to create space for O_2 to bind.[9, 15, 20–22] We propose that the shifts in active site structure may have an additional function as described below.

The reactivity of the Fe(III)-superoxo species with an aromatic ring has not been fully explored, but there are indications that some types of reactions are possible. For example, we and others have proposed that a metal superoxo species can add to a catechol ring to form an alkyl peroxo intermediate in the mechanism of extradiol ring cleaving dioxygenases (Scheme 3A).[73] In this case, we also proposed that the reaction is promoted by electron transfer from the catechol to the iron, so that the iron and catechol have ferrous and radical character, respectively.[74] This, in turn, promotes recombination of the oxygen and substrate radicals to form the alkylperoxo intermediate. In the case of isopenicillin N-synthase, we and others have proposed that an Fe(III)-superoxo is capable of hydrogen atom abstraction from the β-carbon of the cysteinyl moiety of the δ-(L-α-aminoadipoyl)-L-cysteinyl-D-valine (ACV) substrate.[43–45, 75] The energy for such a reaction would be similar to that required for electron abstraction from an aromatic ring. Here again, the Fe(III)-superoxo species can be considered to be somewhat activated by a shift in electron density from the cysteinyl sulfur of ACV bound directly to the iron. One particularly relevant example is found in the tryptophan 2,3-dioxygenase (TDO) and indolamine 2,3 dioxygenase (IDO) systems where electron abstraction from aromatic systems by Fe(II)-O_2 or Fe(III)-superoxo has been computationally and experimentally explored (Scheme 3B).[76–78] For this enzyme class, the iron-oxy system is not significantly activated, but initial attack involving 1- or 2-electron withdrawal from the heterocyclic indole ring, followed by recombination to form an alkylperoxo intermediate is predicted as a first step. Downstream reactions result in dioxygen insertion and indole ring cleavage. Radical reactions with aromatics have also been explored both experimentally and computationally using a diradical form of phthaloyl peroxide in which one radical moiety is proposed to attack an unactivated aryl moiety to form an ester linked aryl radical with only a moderate activation barrier (Scheme 3C).[79]

One route to substrate hydroxylation by BZDO is illustrated in Scheme 4. The current results show that substrate and O_2 binding occur rapidly to BZDO when both the mononuclear iron and Rieske cluster are reduced. Direct radical attack of a potential resulting Fe(III)-superoxo intermediate on the aromatic substrate would yield an Fe(III)-peroxo-aryl radical analogous to the Fe(III)-peroxo-imidazole radical proposed as a feasible

route for the TDO/IDO systems (Scheme 3B). [76–78] In the latter system, the subsequent steps may result in the formation of a substrate epoxide with coincident formation of an Fe(IV)=O at the level of Compound II. Reaction of the high valent oxo species with the epoxide or the carbocation formed upon epoxide ring-opening would result in the dioxygenation reaction and ring opening. In contrast, the BZDO system is able to avoid ring cleavage. This can be achieved by controlling the source of the two electrons required for this phase of the reaction. Rather than utilizing two electrons from the sessile bond (as in the TDO/IDO case), our past results have shown that BZDO uses one from the iron and one from the Rieske cluster.[7, 52] We propose that the high potential Fe(III) formed concurrent with the formation of the putative Fe(III)-peroxo-aryl radical intermediate allows the transfer of an electron from the Rieske cluster. The additional electron would promote homolytic O-O bond cleavage with formation of an intermediate ring epoxide and an Fe(III)-O^-. Opening of the epoxide would yield a carbocation which could abstract the hydroxide anion from the iron to yield the *cis*-diol product without ring opening. In this scenario, the Fe(III)-superoxo species would have to have sufficient Fe(II) character to prevent electron transfer from the Rieske prior to rate limiting attack on the substrate. Other mechanistic scenarios such as heterolytic cleavage of the O-O bond with formation of a high valent iron-oxo intermediate subsequent to formation of the Fe(III)-peroxo-aryl radical species are also possible.

The initial reaction of Fe(III)-superoxo with the aromatic substrate shown in Scheme 4 would depend strongly on susceptibility of the aromatic ring to oxidation, specifically at the position of attack. The current results show that the presence of electron-withdrawing fluorine substituents on the ring deactivate the C(2) position for such an attack. Moreover, the computational evaluation of the effect of the numbers and positions of fluorine atoms on the charge density at the presumed position of attack, C(2), are consistent with this proposed mechanism.

The crystal structure of BZDO has not been reported, making it impossible to explore theoretically any actual reaction coordinate with a requisite level of confidence, but structures of several other RDDs and some intermediates are known. This includes structures of the putative Fe(III)-(H)peroxo intermediate previously assumed by many to be the species that initially attacks the substrate.[13, 15] In all such structures, the distance between the mononuclear iron and the substrate carbon closest to the iron is in the range of 4.2–4.6 Å. This is the expected distance for formation of an aryl-peroxo intermediate. After O-O bond cleavage and electron transfer from the Rieske cluster, the resulting Fe(III)-O^- would be approximately 2.5–3 Å from the nearest substrate carbon. This is not an unreasonable distance for a nucleophilic attack of a Fe(III)-O^- on aryl cation, but the reaction may be further promoted by the return of the Rieske cluster to the oxidized state. Structural studies of 2-oxoquinoline 8-monooxygenase and CarDO show that oxidation of the Rieske cluster forces the mononuclear iron to move approximately 0.5 Å toward the substrate. [15, 20] Such a movement would bring the Fe(III)-O^- and aryl cation in closer proximity and may trigger rapid irreversible completion of the reaction once the electron from the Rieske cluster has been transferred. This reaction would make the rate-limiting

formation of the Fe(III)-peroxo-aryl intermediate appear to be irreversible as we observe, even if it were in fact a reversible process.

Conclusion

Our previous studies have shown that product formation during a single turnover in RDDs results in 1-electron oxidation of each metal center.[7, 52] This stoichiometry together with crystal structures of CarDO and NDO showing a side-on bound peroxo intermediate and our demonstration that the enzymes can use a peroxide shunt to slowly drive catalysis led to the hypothesis that an Fe(III)-(H)peroxo (or HO-Fe(V)=O) species is the reactive species in RDDs. [13, 15, 34, 64] This hypothesis was supported by computations as well as model studies.[36, 55, 80–82] However, the observation here that the apparent rate of the electron transfer from the Rieske cluster required to form the peroxo intermediate depends on the number and position of fluorines introduced into the substrate ring strongly suggests that there is a reaction with substrate prior to electron transfer. The dependence of the rate of this reaction on the electron density at the closest substrate carbon to the iron is consistent with the attacking species being an electrophilic Fe(III)-superoxo. The result of this attack would be an Fe(III)-peroxo-aryl-radical intermediate. While it is possible that the O-O bond cleavage occurs at this stage, we believe that it is unlikely because there is no detectable reaction of any type when only the mononuclear iron is reduced. However, it may also be that the conformation imposed by the oxidized Rieske cluster does not allow substrate and O_2 access to the active site to allow the reaction to initiate. Oxygen bond cleavage after electron transfer from the Rieske cluster would force the reaction onward irreversibly to product formation.

There is little doubt that RDD enzymes can stabilize a reactive Fe(III)-peroxo species as demonstrated in both solution and crystallographic studies. [13, 15, 34] However, the current study suggests that this species is not accessed during normal turnover due to either kinetic or steric constraints. When the intermediate is formed during a single turnover peroxide shunt reaction of fully oxidized BZDO, the product formation reaction occurs on a minute rather than a millisecond time scale. [34]

NDO and other RDDs can catalyze both dioxygenase and adventitious monooxygenase reactions. [83] Use of a radical trap/clock molecule as a monooxygenase substrate for NDO unequivocally demonstrated that a radical intermediate was formed.[84] A radical is unlikely to arise from the attack of an Fe(III)-peroxo intermediate, but it might derive from attack by either an Fe(III)-superoxo species proposed here or an electrophilic HO-Fe(V)=O species hypothesized previously. [84] Indeed, both types of chemistry might occur in the versatile RDD family with the mechanism determined by the reaction type, the oxygen species supplied, the substrate, and the kinetics of individual steps along the reaction coordinate.

Supplementary Material

Refer to Web version on PubMed Central for supplementary material.

Acknowledgments

We thank Simon E. Lewis for the gift of the *Ralstonia eutrophus* strain B9 and Jung-Kul Lee for the gift of the pACYC-*isc* plasmid. We thank Johannes Klein for assistance in NMR analysis.

Funding

This work was supported by NIH grant GM24689 (to J.D.L) and NSF CHE 1361595 (to C.J.C.).

ABBREVIATIONS

RDD	Rieske dearomatizing dioxygenase
benzoate *cis*-diol	(1S,6R)-1,6-*cis*-dihydroxycyclohexa-2,4-diene-1-carboxy acid
BZDR	benzoate 1,2-dioxygenase reductase
BZDO	benzoate 1,2-dioxygenase oxygenase
NDO	naphthalene 1,2-dioxygenase
NBDO	nitrobenzene 1,2-dioxygenase
TPA	tris(2-pyridylmethyl)amine
BPMEN	*N*,*N*'-dimethyl-*N*,*N*'-bis(2-pyridylmethyl)-1,2-diaminoethane
TMC	1,4,8,11-tetramethyl-1,4,8,11-tetraazacyclotetradecane
4-FB	4-fluorobenzoic acid
3,5-FB	3,5-difluorobenzoic acid
3,4,5-FB	3,4,5-trifluorobenzoic acid
RRT	reciprocal relaxation time

REFERENCES

1. Barry S, Challis GL. Mechanism and catalytic diversity of Rieske non-heme iron-dependent oxygenases. ACS Catal. 2013; 3:2362–2370.
2. Gibson DT, Parales RE. Aromatic hydrocarbon dioxygenases in environmental biotechnology. Curr. Opin. Biotechnol. 2000; 11:236–243. [PubMed: 10851146]
3. Aukema KG, Kasinkas L, Aksan A, Wackett LP. Use of silica-encapsulated *Pseudomonas sp*. strain NCIB 9816-4 in biodegradation of novel hydrocarbon ring structures found in hydraulic fracturing waters. Appl. Environ. Microbiol. 2014; 80:4968–4976. [PubMed: 24907321]
4. Lewis SE. Applications of biocatalytic arene ipso, ortho *cis*-dihydroxylation in synthesis. Chem. Commun. 2014; 50:2821–2830.
5. Jenkins GN, Ribbons DW, Widdowson DA, Slawin AMZ, Williams DJ. Synthetic application of biotransformations: absolute stereochemistry and Diels-Alder reactions of the (1S,2R)-1,2-dihydroxycyclohexa-3,5-diene-1-carboxylic acid from *Pseudomonas putida* . J. Chem. Soc., Perkin Trans. 1995; 1:2647–2655.
6. Myers AG, Siegel DR, Buzard DJ, Charest MG. Synthesis of a broad array of highly functionalized, enantiomerically pure cyclohexanecarboxylic acid derivatives by microbial dihydroxylation of benzoic acid and subsequent oxidative and rearrangement reactions. Org. Lett. 2001; 3:2923–2926. [PubMed: 11529791]
7. Wolfe MD, Altier DJ, Stubna A, Popescu CV, Münck E, Lipscomb JD. Benzoate 1,2-dioxygenase from *Pseudomonas putida*: Single turnover kinetics and regulation of a two-component Rieske dioxygenase. Biochemistry. 2002; 41:9611–9626. [PubMed: 12135383]

8. Koehntop KD, Emerson JP, Que L Jr. The 2-His-1-carboxylate facial triad: a versatile platform for dioxygen activation by mononuclear non-heme iron(II) enzymes. J. Biol. Inorg. Chem. 2005; 10:87–93. [PubMed: 15739104]

9. Ohta T, Chakrabarty S, Lipscomb JD, Solomon EI. Near-IR MCD of the nonheme ferrous active site in naphthalene 1,2-dioxygenase: Correlation to crystallography and structural insight into the mechanism of Rieske dioxygenases. J. Am. Chem. Soc. 2008; 130:1601–1610. [PubMed: 18189388]

10. Ferraro DJ, Gakhar L, Ramaswamy S. Rieske business: Structure-function of Rieske non-heme oxygenases. Biochem. Biophys. Res. Commun. 2005; 338:175–190. [PubMed: 16168954]

11. Kauppi B, Lee K, Carredano E, Parales RE, Gibson DT, Eklund H, Ramaswamy S. Structure of an aromatic-ring-hydroxylating dioxygenase-naphthalene 1,2-dioxygenase. Structure. 1998; 6:571–586. [PubMed: 9634695]

12. Carredano E, Karlsson A, Kauppi B, Choudhury D, Parales RE, Parales JV, Lee K, Gibson DT, Eklund H, Ramaswamy S. Substrate binding site of naphthalene 1,2-dioxygenase: Functional implications of indole binding. J. Mol. Biol. 2000; 296:701–712. [PubMed: 10669618]

13. Karlsson A, Parales JV, Parales RE, Gibson DT, Eklund H, Ramaswamy S. Crystal structure of naphthalene dioxygenase: Side-on binding of dioxygen to iron. Science. 2003; 299:1039–1042. [PubMed: 12586937]

14. Friemann R, Ivkovic-Jensen MM, Lessner DJ, Yu C-L, Gibson DT, Parales RE, Eklund H, Ramaswamy S. Structural insight into the dioxygenation of nitroarene compounds: the crystal structure of nitrobenzene dioxygenase. J. Mol. Biol. 2005; 348:1139–1151. [PubMed: 15854650]

15. Ashikawa Y, Fujimoto Z, Usami Y, Inoue K, Noguchi H, Yamane H, Nojiri H. Structural insight into the substrate- and dioxygen-binding manner in the catalytic cycle of Rieske nonheme iron oxygenase system, carbazole 1,9a–dioxygenase. BMC Structural Biology. 2012; 12:15. [PubMed: 22727022]

16. Parales RE, Parales JV, Gibson DT. Aspartate 205 in the catalytic domain of naphthalene dioxygenase is essential for activity. J. Bacteriol. 1999; 181:1831–1837. [PubMed: 10074076]

17. Beharry ZM, Eby DM, Coulter ED, Viswanathan R, Neidle EL, Phillips RS, Kurtz DM Jr. Histidine ligand protonation and redox potential in the Rieske dioxygenases: Role of a conserved aspartate in anthranilate 1,2-dioxygenase. Biochemistry. 2003; 42:13625–13636. [PubMed: 14622009]

18. Pinto A, Tarasev M, Ballou DP. Substitutions of the “bridging” aspartate 178 result in profound changes in the reactivity of the Rieske center of phthalate dioxygenase. Biochemistry. 2006; 45:9032–9041. [PubMed: 16866348]

19. Tarasev M, Pinto A, Kim D, Elliott SJ, Ballou DP. The “bridging” aspartate 178 in phthalate dioxygenase facilitates interactions between the Rieske center and the iron(II)-mononuclear center. Biochemistry. 2006; 45:10208–10216. [PubMed: 16922496]

20. Martins BM, Svetlitchnaia T, Dobbek H. 2-Oxoquinoline 8-monooxygenase oxygenase component: active site modulation by Rieske-[2Fe-2S] center oxidation/reduction. Structure. 2005; 13:817–824. [PubMed: 15893671]

21. Yang T-C, Wolfe MD, Neibergall MB, Mekmouche Y, Lipscomb JD, Hoffman BM. Substrate binding to NO-ferro-naphthalene 1,2-dioxygenase studied by high-resolution Q-band pulsed ^{2}H-ENDOR spectroscopy. J. Am. Chem. Soc. 2003; 125:7056–7066. [PubMed: 12783560]

22. Yang T-C, Wolfe MD, Neibergall MB, Mekmouche Y, Lipscomb JD, Hoffman BM. Modulation of substrate binding to naphthalene 1,2-dioxygenase by Rieske cluster reduction/oxidation. J. Am. Chem. Soc. 2003; 125:2034–2035. [PubMed: 12590516]

23. Solomon EI, Light KM, Liu LV, Srnec M, Wong SD. Geometric and electronic structure contributions to function in non-heme iron enzymes. Acc. Chem. Res. 2013; 46:2725–2739. [PubMed: 24070107]

24. Kovaleva EG, Lipscomb JD. Versatility of biological non-heme Fe(II) centers in oxygen activation reactions. Nat. Chem. Biol. 2008; 4:186–193. [PubMed: 18277980]

25. Dalton H. Oxidation of hydrocarbons by methane monooxygenase from a variety of microbes. Adv. Appl. Microbiol. 1980; 26:71–87.

26. Tyson CA, Lipscomb JD, Gunsalus IC. The role of putidaredoxin and $P450_{cam}$ in methylene hydroxylation. J. Biol. Chem. 1972; 247:5777–5784. [PubMed: 4341491]
27. Ortiz de Montellano, PR. Cytochrome P450 : Structure, Mechanism, and Biochemistry. New York: Plenum Press; 1995.
28. Zhou N-Y, Al-Dulayymi J, Baird MS, Williams PA. Salicylate 5-hydroxylase from *Ralstonia* sp. strain U2: a monooxygenase with close relationships to and shared electron transport proteins with naphthalene dioxygenase. J. Bacteriol. 2002; 184:1547–1555. [PubMed: 11872705]
29. Tinberg CE, Lippard SJ. Dioxygen activation in soluble methane monooxygenase. Acc. Chem. Res. 2011; 44:280–288. [PubMed: 21391602]
30. Liu KE, Valentine AM, Wang DL, Huynh BH, Edmondson DE, Salifoglou A, Lippard SJ. Kinetic and spectroscopic characterization of intermediates and component interactions in reactions of methane monooxygenase from *Methylococcus capsulatus* (Bath). J. Am. Chem. Soc. 1995; 117:10174–10185.
31. Lee SK, Lipscomb JD. Oxygen activation catalyzed by methane monooxygenase hydroxylase component: Proton delivery during the O-O bond cleavage steps. Biochemistry. 1999; 38:4423–4432. [PubMed: 10194363]
32. Davydov R, Makris TM, Kofman V, Werst DE, Sligar SG, Hoffman BM. Hydroxylation of camphor by reduced oxy-cytochrome $P450_{cam}$: Mechanistic implications of EPR and ENDOR studies of catalytic intermediates in native and mutant enzymes. J. Am. Chem. Soc. 2001; 123:1403–1415. [PubMed: 11456714]
33. Denisov IG, Makris TM, Sligar SG, Schlichting I. Structure and chemistry of cytochrome P450. Chem. Rev. 2005; 105:2253–2277. [PubMed: 15941214]
34. Neibergall MB, Stubna A, Mekmouche Y, Münck E, Lipscomb JD. Hydrogen peroxide dependent *cis*-dihydroxylation of benzoate by fully oxidized benzoate 1,2-dioxygenase. Biochemistry. 2007; 46:8004–8016. [PubMed: 17567152]
35. Bassan A, Blomberg MRA, Siegbahn PEM. A theoretical study of the *cis*-dihydroxylation mechanism in naphthalene 1,2-dioxygenase. J. Biol. Inorg. Chem. 2004; 9:439–452. [PubMed: 15042436]
36. Pabis A, Geronimo I, Paneth P. A DFT study of the *cis*-dihydroxylation of nitroaromatic compounds catalyzed by nitrobenzene dioxygenase. J. Phys. Chem. B. 2014; 118:3245–3256. [PubMed: 24624972]
37. Chen K, Costas M, Kim J, Tipton AK, Que L Jr. Olefin *cis*-dihydroxylation versus epoxidation by non-heme iron catalysts: two faces of an Fe^{III}-OOH coin. J. Am. Chem. Soc. 2002; 124:3026–3035. [PubMed: 11902894]
38. Prat I, Mathieson JS, Guell M, Ribas X, Luis JM, Cronin L, Costas M. Observation of Fe(V)=O using variable-temperature mass spectrometry and its enzyme-like C-H and C=C oxidation reactions. Nat. Chem. 2011; 3:788–793. [PubMed: 21941251]
39. Oloo WN, Fielding AJ, Que L Jr. Rate-determining water-assisted O-O bond cleavage of an Fe(III)-OOH intermediate in a bio-inspired nonheme iron-catalyzed oxidation. J. Am. Chem. Soc. 2013; 135:6438–6441. [PubMed: 23594282]
40. Liu LV, Hong S, Cho J, Nam W, Solomon EI. Comparison of high-spin and low-spin nonheme Fe(III)-OOH complexes in O-O bond homolysis and H-atom abstraction reactivities. J. Am. Chem. Soc. 2013; 135:3286–3299. [PubMed: 23368958]
41. Mbughuni MM, Chakrabarti M, Hayden JA, Meier KK, Dalluge JJ, Hendrich MP, Münck E, Lipscomb JD. Oxy-intermediates of homoprotocatechuate 2,3-dioxygenase: Facile electron transfer between substrates. Biochemistry. 2011; 50:10262–10274. [PubMed: 22011290]
42. Mbughuni MM, Chakrabarti M, Hayden JA, Bominaar EL, Hendrich MP, Münck E, Lipscomb JD. Trapping and spectroscopic characterization of an Fe^{III}-superoxo intermediate from a nonheme mononuclear iron-containing enzyme. Proc. Natl. Acad. Sci. USA. 2010; 107:16788–16793. [PubMed: 20837547]
43. Brown CD, Neidig ML, Neibergall MB, Lipscomb JD, Solomon EI. VTVH-MCD and DFT studies of thiolate bonding to $\{FeNO\}^7/\{FeO_2\}^8$ complexes of isopenicillin N synthase: substrate determination of oxidase versus oxygenase activity in nonheme Fe enzymes. J. Am. Chem. Soc. 2007; 129:7427–7438. [PubMed: 17506560]

44. van der Donk WA, Krebs C, Bollinger JM Jr. Substrate activation by iron superoxo intermediates. Curr. Opin. Struct. Biol. 2010; 20:673–683. [PubMed: 20951572]
45. Bollinger JM Jr, Krebs C. Enzymatic C-H activation by metal-superoxo intermediates. Curr. Opin. Chem. Biol. 2007; 11:151–158. [PubMed: 17374503]
46. Zhao Y, Truhlar DG. The M06 suite of density functionals for main group thermochemistry, thermochemical kinetics, noncovalent interactions, excited states, and transition elements: two new functionals and systematic testing of four M06-class functionals and 12 other functionals. Theor. Chem. Acc. 2008; 120:215–241.
47. Hehre, WJ.; Random, L.; Schleyer, PvR; Pople, JA. Ab Initio Molecular Orbital Theory. New York: Wiley; 1986.
48. Marenich AV, Cramer CJ, Truhlar DG. Universal solvation model based on solute electron density and on a continuum model of the solvent defined by the bulk dielectric constant and atomic surface tensions. J. Phys. Chem. B. 2009; 113:6378–6396. [PubMed: 19366259]
49. Marenich AV, Jerome SV, Cramer CJ, Truhlar DG. Charge model 5: An extension of Hirshfeld population analysis for the accurate description of molecular interactions in gaseous and condensed phases. J. Chem. Theory Comput. 2012; 8:527–541.
50. Frisch, MJ.; Trucks, GW.; Schlegel, HB.; Scuseria, GE.; Robb, MA.; Cheeseman, JR.; Scalmani, G.; Barone, V.; Mennucci, B.; Petersson, GA.; Nakatsuji, H.; Caricato, M.; Li, X.; Hratchian, HP.; Izmaylov, AF.; Bloino, J.; Zheng, G.; Sonnenberg, JL.; Hada, M.; Ehara, M.; Toyota, K.; Fukuda, R.; Hasegawa, J.; Ishida, M.; Nakajima, T.; Honda, Y.; Kitao, O.; Nakai, H.; Vreven, T.; Montgomery, JA.; Peralta, JE.; Ogliaro, F.; Bearpark, M.; Heyd, JJ.; Brothers, E.; Kudin, KN.; Staroverov, VN.; Kobayashi, R.; Normand, J.; Raghavachari, K.; Rendell, A.; Burant, JC.; Iyengar, SS.; Tomasi, J.; Cossi, M.; Rega, N.; Millam, JM.; Klene, M.; Knox, JE.; Cross, JB.; Bakken, V.; Adamo, C.; Jaramillo, J.; Gomperts, R.; Stratmann, RE.; Yazyev, O.; Austin, AJ.; Cammi, R.; Pomelli, C.; Ochterski, JW.; Martin, RL.; Morokuma, K.; Zakrzewski, VG.; Voth, GA.; Salvador, P.; Dannenberg, JJ.; Dapprich, S.; Daniels, AD.; Farkas, Ö.; Foresman, JB.; Ortiz, JV.; Cioslowski, J.; Fox, DJ. Gaussian 09, Revision C.01. Wallingford, CT: Gaussian Inc; 2010.
51. Marenich, AV.; Cramer, CJ.; Truhlar, DG. CM5PAC. Minneapolis: University of Minnesota; 2011.
52. Wolfe MD, Parales JV, Gibson DT, Lipscomb JD. Single turnover chemistry and regulation of O_2 activation by the oxygenase component of naphthalene 1,2-dioxygenase. J. Biol. Chem. 2001; 276:1945–1953. [PubMed: 11056161]
53. Bernhardt FH, Ruf HH, Ehrig H. A 4-methoxybenzoate monooxygenase system from *Pseudomonas putida*. Circular dichroism studies on the iron--sulfur protein. FEBS Lett. 1974; 43:53–55. [PubMed: 4850360]
54. Twilfer H, Bernhardt FH, Gersonde K. Dioxygen-activating iron center in putidamonooxin. Electron spin resonance investigation of the nitrosylated putidamonooxin. Eur. J. Biochem. 1985; 147:171–176. [PubMed: 2982606]
55. Bassan A, Blomberg MRA, Borowski T, Siegbahn PEM. Oxygen activation by Rieske non-heme iron oxygenases, a theoretical insight. J. Phys. Chem. B. 2004; 108:13031–13041.
56. Liu Y, Nesheim JC, Lee S-K, Lipscomb JD. Gating effects of component B on oxygen activation by the methane monooxygenase hydroxylase component. J. Biol. Chem. 1995; 270:24662–24665. [PubMed: 7559577]
57. DuBois JL, Klinman JP. The nature of O_2 reactivity leading to topa quinone in the copper amine oxidase from *Hansenula polymorpha* and its relationship to catalytic turnover. Biochemistry. 2005; 44:11381–11388. [PubMed: 16114875]
58. Orville AM, Lipscomb JD, Ohlendorf DH. Crystal structures of substrate and substrate analog complexes of protocatechuate 3,4-dioxygenase: endogenous Fe^{3+} ligand displacement in response to substrate binding. Biochemistry. 1997; 36:10052–10066. [PubMed: 9254600]
59. Karlsson A, Parales JV, Parales RE, Gibson DT, Eklund H, Ramaswamy S. NO binding to naphthalene dioxygenase. J. Biol. Inorg. Chem. 2005; 10:483–489. [PubMed: 15942729]
60. Orville AM, Lipscomb JD. Simultaneous binding of nitric oxide and isotopically labeled substrates or inhibitors by reduced protocatechuate 3,4-dioxygenase. J. Biol. Chem. 1993; 268:8596–8607. [PubMed: 8386164]

61. Arciero DM, Lipscomb JD, Huynh BH, Kent TA, Münck E. EPR and Mössbauer studies of protocatechuate 4,5-dioxygenase. Characterization of a new Fe^{2+} environment. J. Biol. Chem. 1983; 258:14981–14991. [PubMed: 6317682]
62. Schenk G, Pau MYM, Solomon EI. Comparison between the geometric and electronic structures and reactivities of $\{FeNO\}^7$ and $\{FeO_2\}^8$ complexes: A density functional theory study. J. Am. Chem. Soc. 2004; 126:505–515. [PubMed: 14719948]
63. Tinberg CE, Tonzetich ZJ, Wang H, Do LH, Yoda Y, Cramer SP, Lippard SJ. Characterization of iron dinitrosyl species formed in the reaction of nitric oxide with a biological Rieske center. J. Am. Chem. Soc. 2010; 132:18168–18176. [PubMed: 21133361]
64. Wolfe MD, Lipscomb JD. Hydrogen peroxide-coupled *cis*-diol formation catalyzed by naphthalene 1,2-dioxygenase. J. Biol. Chem. 2003; 278:829–835. [PubMed: 12403773]
65. Bugg TDH, Ramaswamy S. Non-heme iron-dependent dioxygenases: unravelling catalytic mechanisms for complex enzymatic oxidations. Curr. Opin. Chem. Biol. 2008; 12:134–140. [PubMed: 18249197]
66. Shaik S, Cohen S, Wang Y, Chen H, Kumar D, Thiel W. P450 enzymes: Their structure, reactivity, and selectivities modeled by QM/MM calculations. Chem. Rev. 2010; 110:949–1017. [PubMed: 19813749]
67. Wallar BJ, Lipscomb JD. Dioxygen activation by enzymes containing binuclear non-heme iron clusters. Chem. Rev. 1996; 96:2625–2657. [PubMed: 11848839]
68. Kovaleva EG, Neibergall MB, Chakrabarty S, Lipscomb JD. Finding intermediates in the O_2 activation pathways of non-heme iron oxygenases. Acc. Chem. Res. 2007; 40:475–483. [PubMed: 17567087]
69. Tarasev M, Rhames F, Ballou DP. Rates of the phthalate dioxygenase reaction with oxygen are dramatically increased by interactions with phthalate and phthalate oxygenase reductase. Biochemistry. 2004; 43:12799–12808. [PubMed: 15461452]
70. Lee K. Benzene-induced uncoupling of naphthalene dioxygenase activity and enzyme inactivation by production of hydrogen peroxide. J. Bacteriol. 1999; 181:2719–2725. [PubMed: 10217759]
71. Twilfer H, Sandfort G, Bernhardt F-H. Substrate and solvent isotope effects on the fate of the active oxygen species in substrate-modulated reactions of putidamonooxin. Eur. J. Biochem. 2000; 267:5926–5934. [PubMed: 10998052]
72. Perez-Pantoja D, Nikel PI, Chavarria M, de Lorenzo V. Endogenous stress caused by faulty oxidation reactions fosters evolution of 2,4-dinitrotoluene-degrading bacteria. PLoS Genet. 2013; 9:e1003764. [PubMed: 24009532]
73. Lipscomb JD. Mechanism of extradiol aromatic ring-cleaving dioxygenases. Curr. Opin. Struct. Biol. 2008; 18:644–649. [PubMed: 19007887]
74. Kovaleva EG, Lipscomb JD. Crystal structures of Fe^{2+} dioxygenase superoxo, alkylperoxo, and bound product intermediates. Science. 2007; 316:453–457. [PubMed: 17446402]
75. Lundberg M, Siegbahn PEM, Morokuma K. The mechanism for isopenicillin N synthase from density-functional modeling highlights the similarities with other enzymes in the 2-His-1-carboxylate family. Biochemistry. 2008; 47:1031–1042. [PubMed: 18163649]
76. Capece L, Lewis-Ballester A, Yeh S-R, Estrin DA, Marti MA. Complete reaction mechanism of indoleamine 2,3-dioxygenase as revealed by QM/MM simulations. J. Phys. Chem. B. 2012; 116:1401–1413. [PubMed: 22196056]
77. Chung LW, Li X, Sugimoto H, Shiro Y, Morokuma K. ONIOM study on a missing piece in our understanding of heme chemistry: Bacterial tryptophan 2,3-dioxygenase with dual oxidants. J. Am. Chem. Soc. 2010; 132:11993–12005. [PubMed: 20698527]
78. Basran J, Efimov I, Chauhan N, Thackray SJ, Krupa JL, Eaton G, Griffith GA, Mowat CG, Handa S, Raven EL. The mechanism of formation of N-formylkynurenine by heme dioxygenases. J. Am. Chem. Soc. 2011; 133:16251–16257. [PubMed: 21892828]
79. Yuan C, Liang Y, Hernandez T, Berriochoa A, Houk KN, Siegel D. Metal-free oxidation of aromatic carbon-hydrogen bonds through a reverse-rebound mechanism. Nature. 2013; 499:192–196. [PubMed: 23846658]

80. Das P, Que L Jr. Iron catalyzed competitive olefin oxidation and ipso-hydroxylation of benzoic acids: Further evidence for an Fe^{V}=O oxidant. Inorg. Chem. 2010; 49:9479–9485. [PubMed: 20866083]

81. Lyakin OY, Prat I, Bryliakov KP, Costas M, Talsi EP. EPR detection of Fe(V)=O active species in nonheme iron-catalyzed oxidations. Catal. Commun. 2012; 29:105–108.

82. Gomez L, Canta M, Font D, Prat I, Ribas X, Costas M. Regioselective oxidation of nonactivated alkyl C-H groups using highly structured non-heme iron catalysts. J. Org. Chem. 2013; 78:1421–1433. [PubMed: 23301685]

83. Gibson DT, Resnick SM, Lee K, Brand JM, Torok DS, Wackett LP, Schocken MJ, Haigler BE. Desaturation, dioxygenation, and monooxygenation reactions catalyzed by naphthalene dioxygenase from *Pseudomonas sp*. strain 9816-4. J. Bacteriol. 1995; 177:2615–2621. [PubMed: 7751268]

84. Chakrabarty S, Austin RN, Deng D, Groves JT, Lipscomb JD. Radical intermediates in monooxygenase reactions of Rieske dioxygenases. J. Am. Chem. Soc. 2007; 129:3514–3515. [PubMed: 17341076]

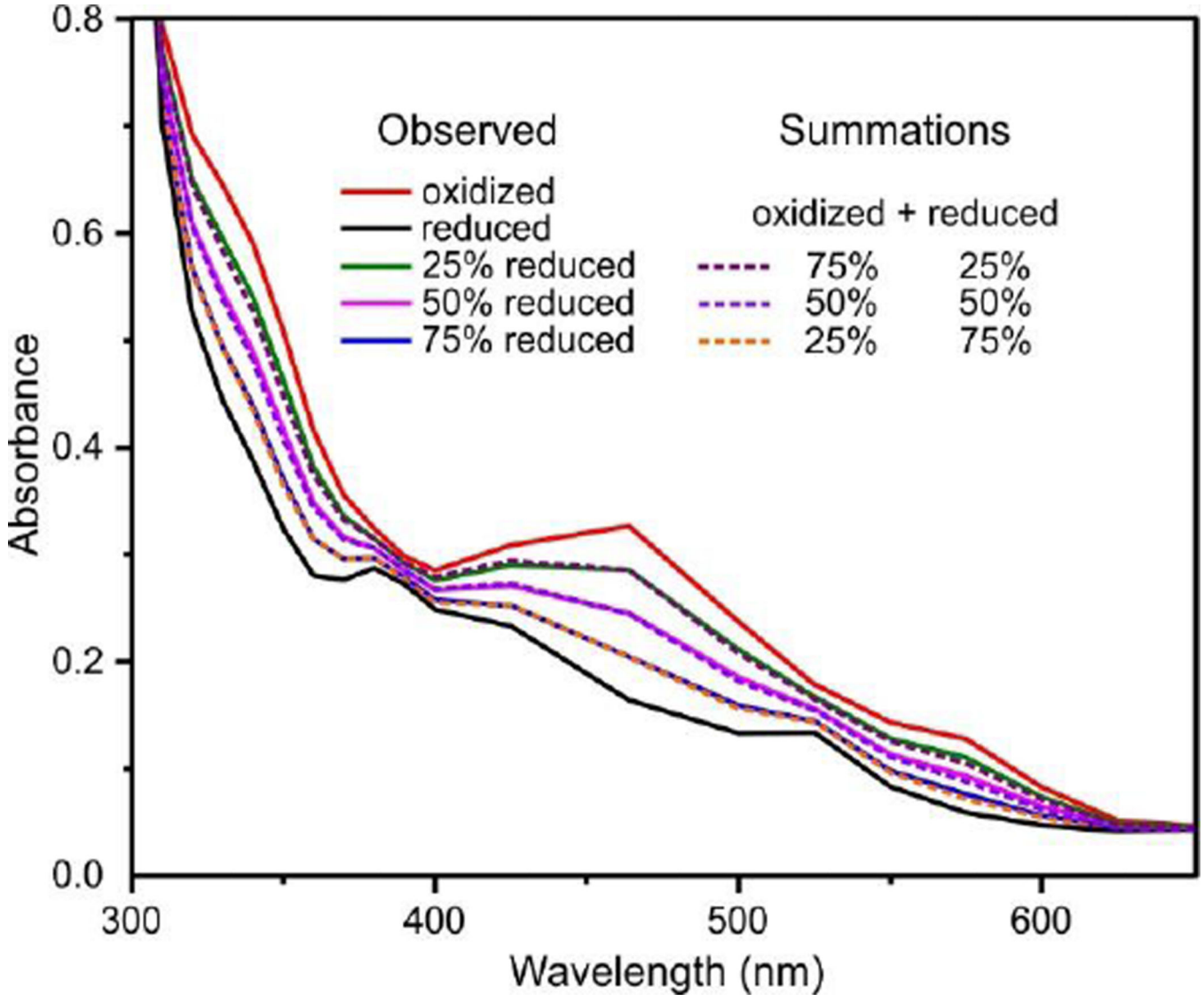

Figure 1.

The optical changes during a single turnover with benzoate are well-accounted for by linear summations of the spectra of the reduced and oxidized Rieske cluster. Selected optical spectra observed after reduced BZDO (100 μM) was mixed with an O_2 saturated reaction buffer containing benzoate (20 mM) at 4 °C in a stopped-flow spectrophotometer. The spectra are combinations of 21 single wavelength time courses collected from 300 −725 nm. The simulated spectra were calculated by summing the indicated fractions of the fully reduced and fully oxidized Rieske cluster spectra.

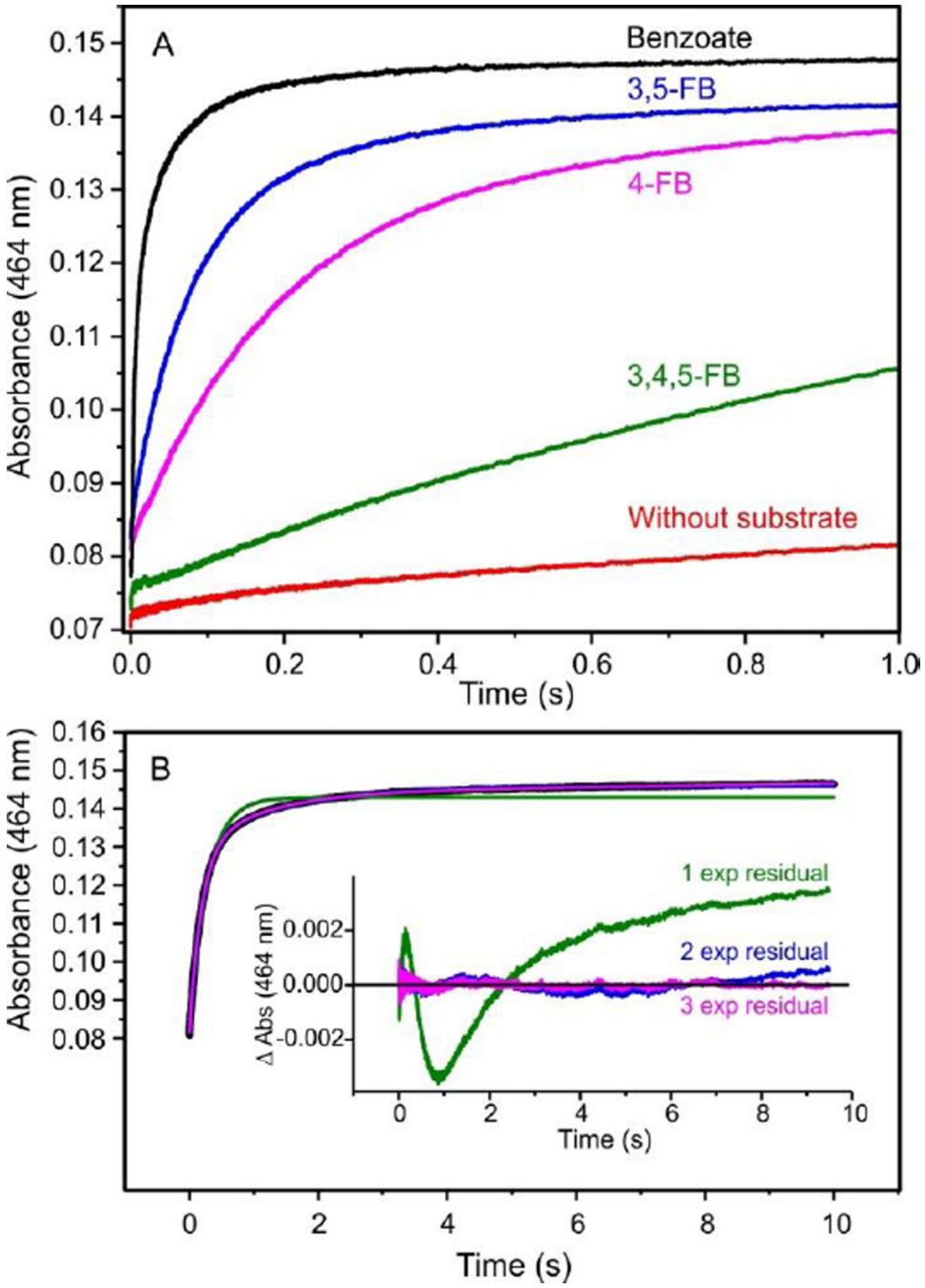

Figure 2.

Rieske cluster oxidation rates during a single turnover depend upon the type of substrate present. (A) Optical change at 464 nm when reduced BZDO (60 μM) was mixed with an O_2 saturated reaction buffer containing the indicated substrate (5 mM) at 4 °C in a stopped-flow spectrophotometer. (B) The resulting optical change at 464 nm with 4-fluorobenzoate and residuals from single, double, and triple exponential function fits.

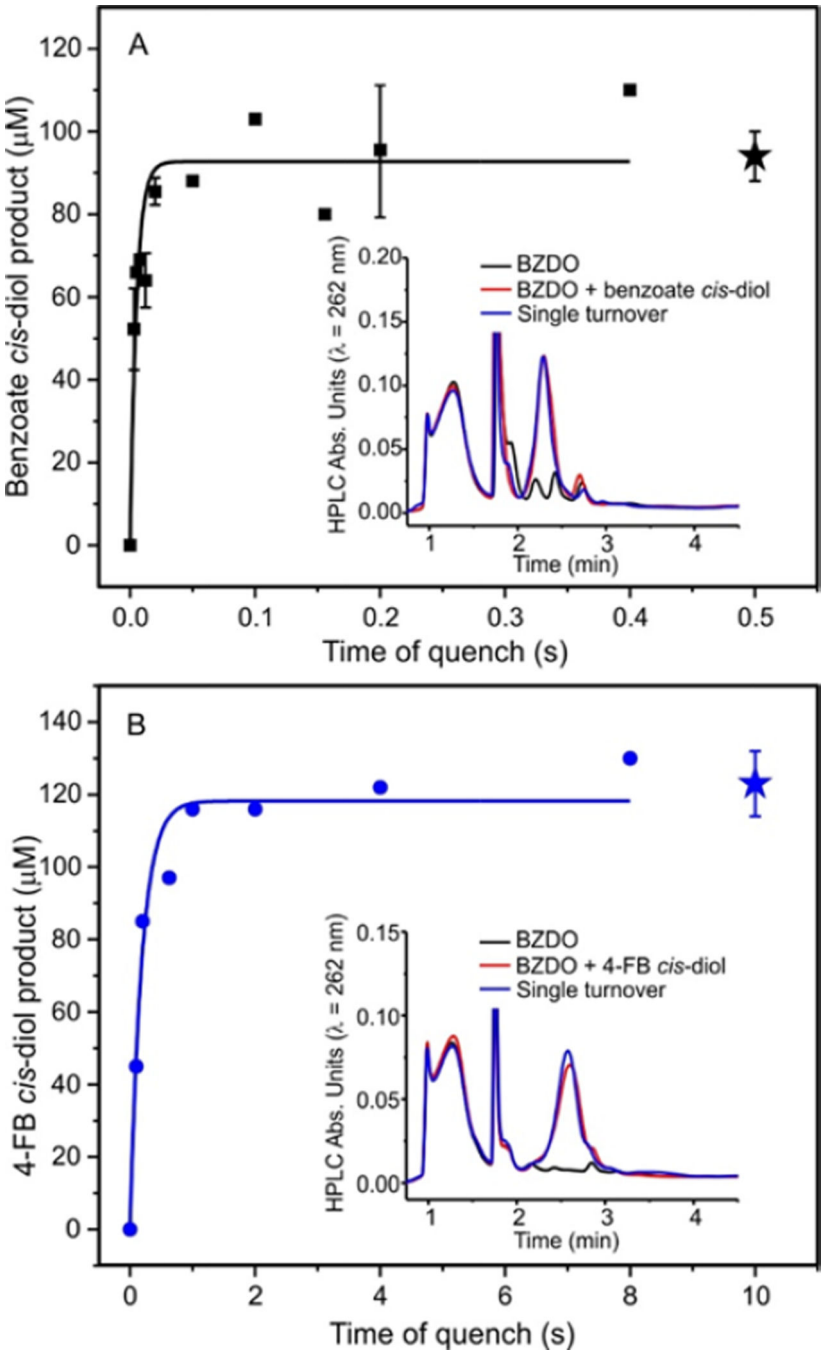

Figure 3.

Product analysis of single turnover reactions shows a correlation with the fast phase of Rieske cluster oxidation. Reduced BZDO (400 μM) was rapidly mixed 1:1 with O_2 saturated reaction buffer containing (A) benzoate (10 mM) or (B) 4-FB (10 mM) and chemically quenched as described in the Experimental Procedures. The yield at the end of the reaction (≥ 4 min) is shown by a star. The product formation time course can be fit to a single exponential equation for each substrate (solid line), yielding the k_{obs}. In each case, a single new HPLC peak consistent with an authentic standard of the *cis*-diol product is observed

(insets). For replicated points, $n \geq 3$ and the errors bars represent 1 standard deviation of the mean.

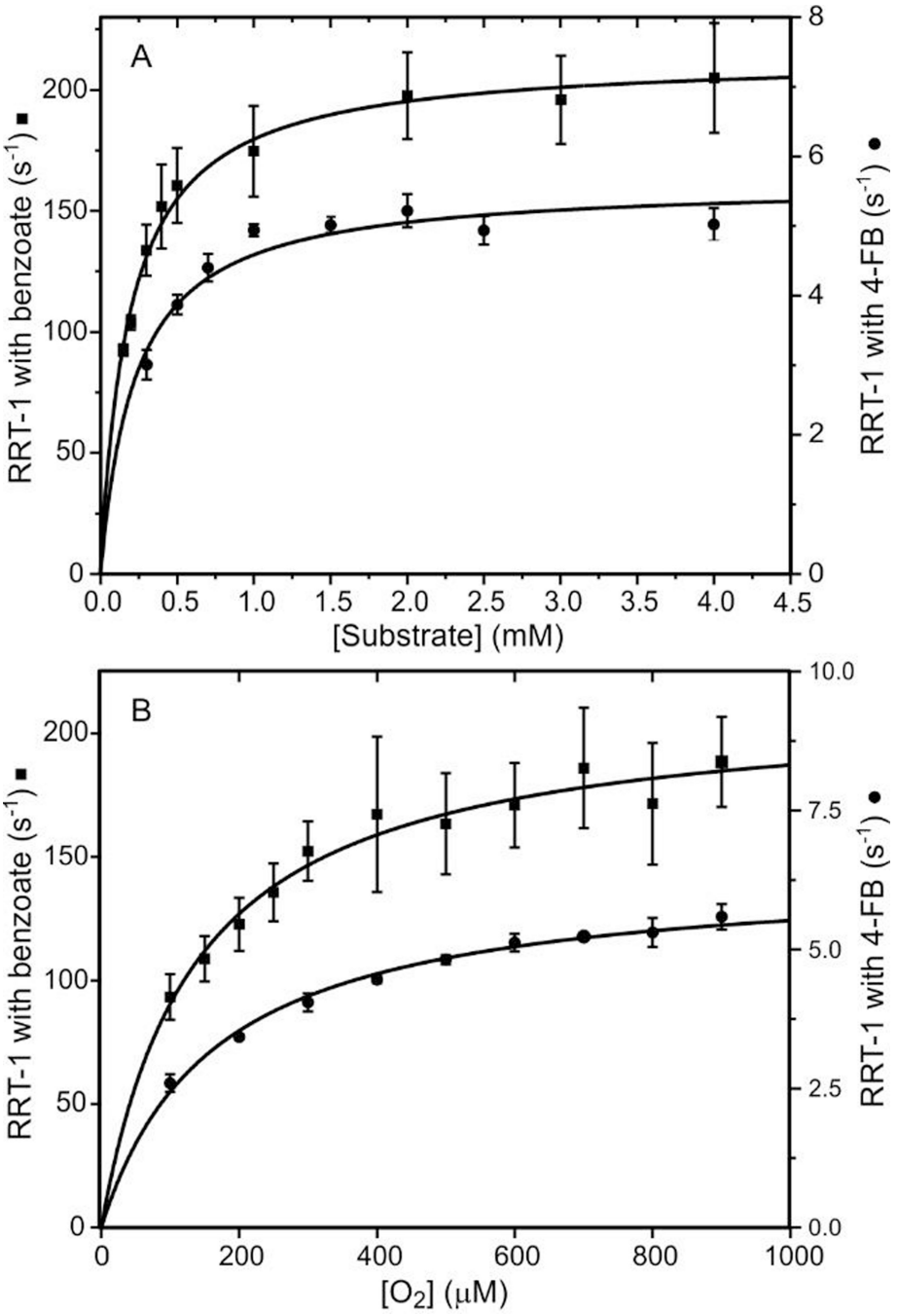

Figure 4.

Substrate and O_2 concentration dependence of RRT-1 reveals a common subsequent slow step. Reduced BZDO (60 μM) was mixed 1:1 in a stopped-flow spectrophotometer with reaction buffer containing either (A) O_2 (saturated solution at 4 °C ≈ 1.8 mM) and varied concentrations of benzoate or 4-FB, or (B) varied concentrations of O_2 and benzoate (5 mM) or 4-FB (5 mM). RRT-1 from multiexponential fitting of stopped-flow traces ($n \geq 6$ and 4 for the reaction of benzoate and 4FB, respectively) was plotted vs (A) substrate or (B) O_2 concentration. Reported error of each point is one standard deviation of the mean. K_d and

$k_{forward}$ values were determined by fitting the data to a hyperbolic function (solid curve) and are reported in Table 2.

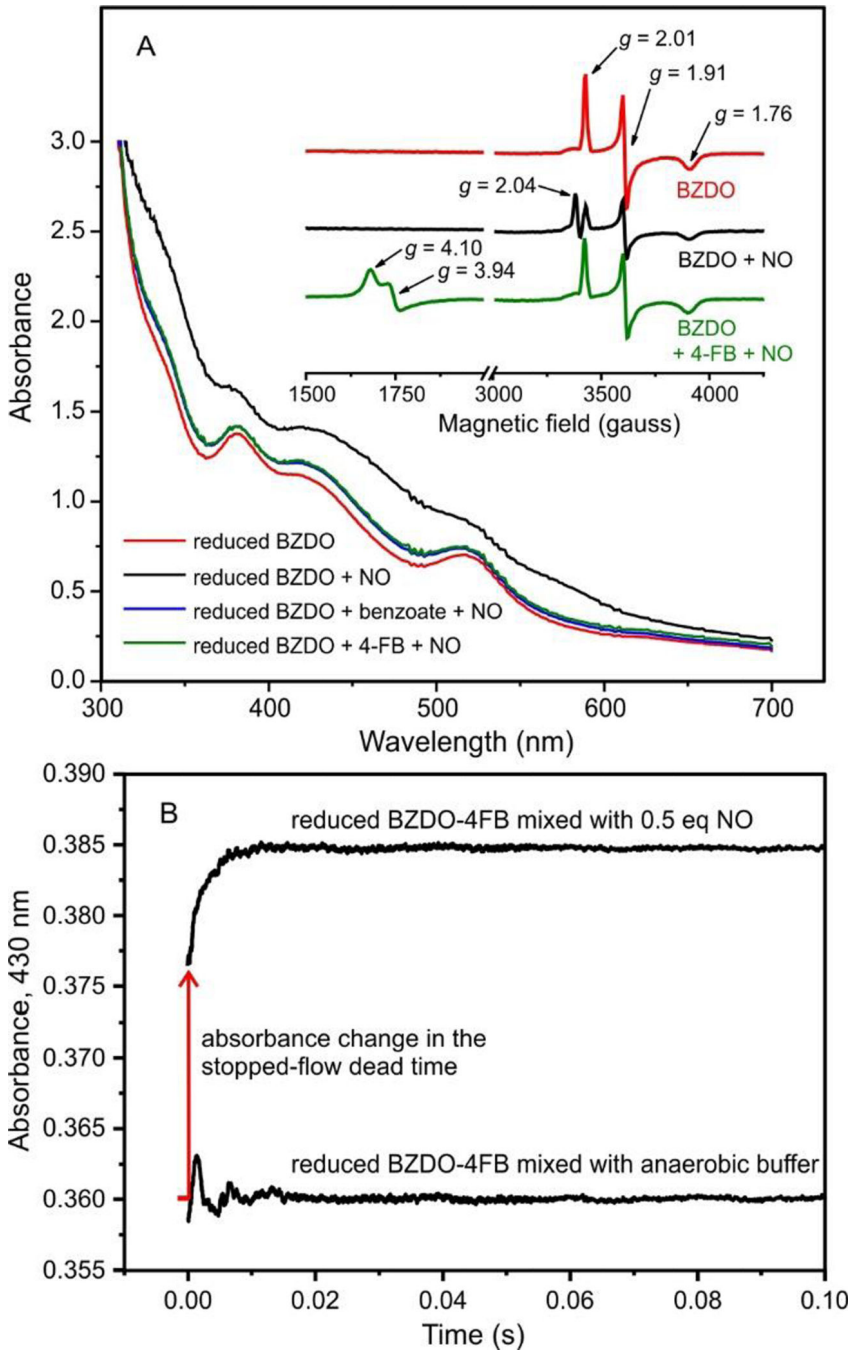

Figure 5.

NO binds rapidly to the mononuclear Fe(II) in the substrate complex. (A) The optical spectra of reduced BZDO (250 μM) with or without benzoate (50 mM) or 4-FB (50 mM) are shown 15 min after the addition of NO (~ 0.5 equivalents relative to BZDO sites). In the absence of substrate, the large change in electronic absorption is caused by NO binding to the Rieske cluster as can be observed by the attenuation of the $S = ½$ ($g = 2.01$, 1.91, and 1.76) EPR signal (inset) from the reduced Rieske cluster and formation of a new signal at $g = 2.04$. In the presence of benzoate or 4-FB, the NO adduct of the mononuclear iron is

formed as shown by the appearance of the characteristic $S = 3/2$ ($g = 4.10$ and 3.94) EPR signal. Conditions: microwave power, 0.2 mW; temperature, 20 K; microwave frequency, 9.64 GHz. (B) A solution of reduced BZDO (200 μM) and 4-FB (1 mM) was mixed 1:1 in a stopped-flow instrument with anaerobic reaction buffer or anaerobic buffer containing NO (~ 0.5 eq relative to BZDO). Formation of the Fe(III)-NO adduct was monitored by the increase in absorption at 430 nm. The same experiment using benzoate in place of 4-FB gave indistinguishable results.

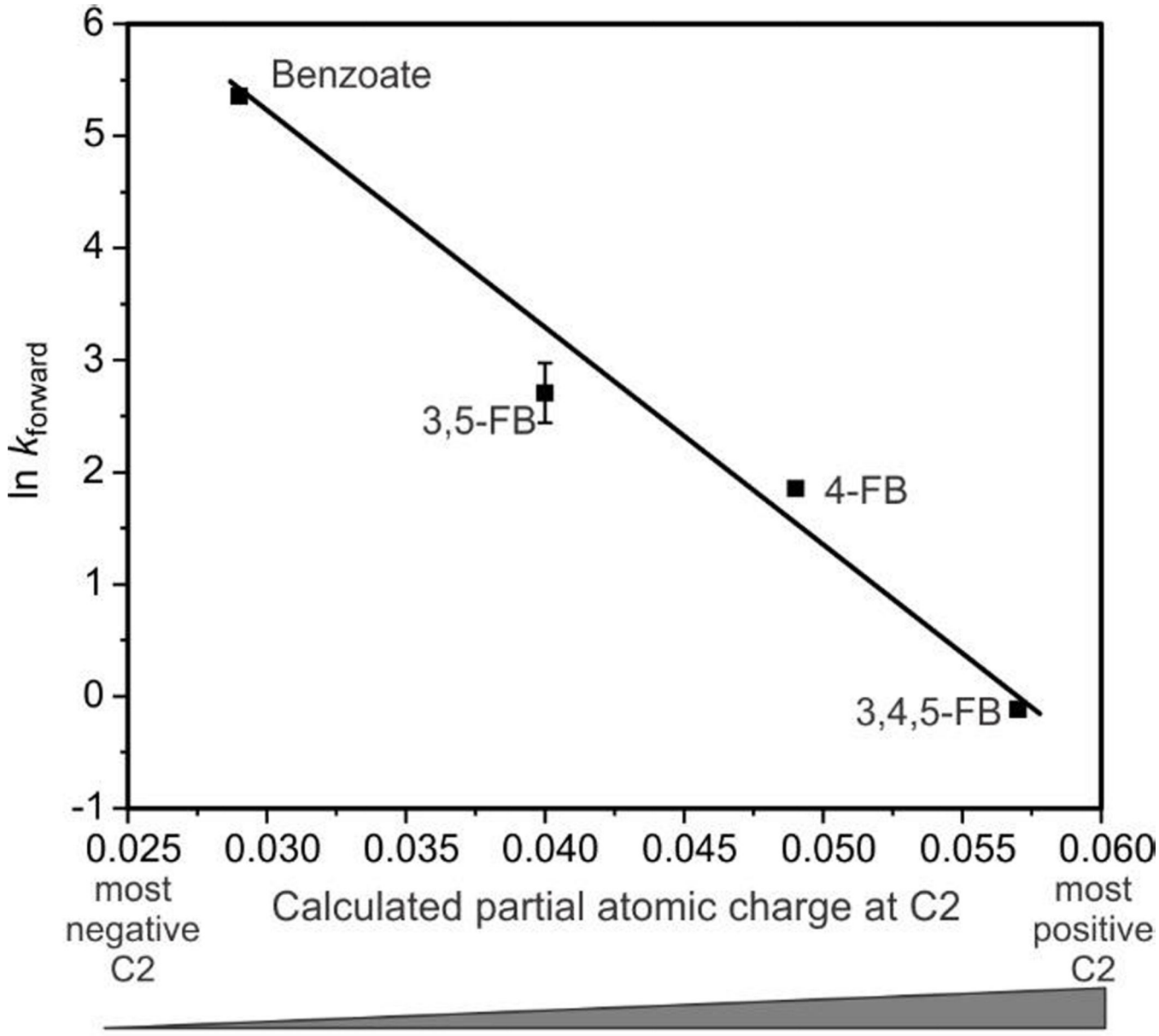

Figure 6.

The logarithm of the rate of Rieske cluster oxidation is proportional to the calculated partial group charge at C(2)–H of the substrates tested. A linear trend is observed showing RRT-1 decreases as the electron density at the C(2)–H group decreases.

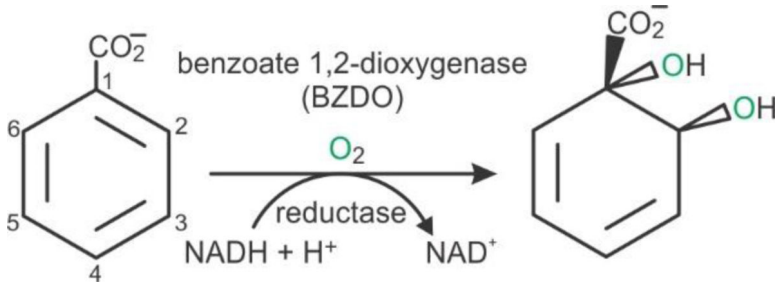

Scheme 1.
Reaction of the RDD Benzoate 1,2-Dioxygenase

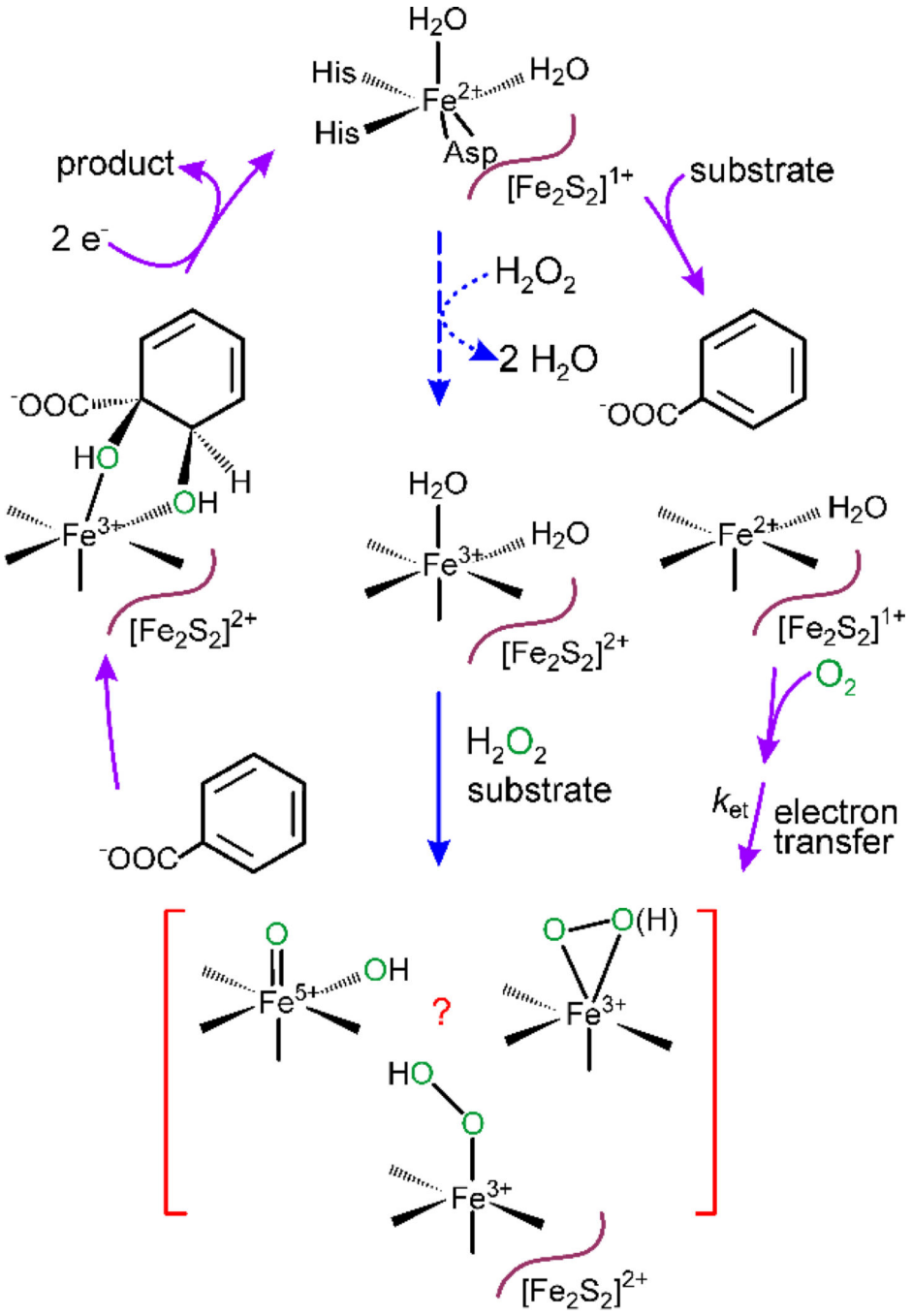

Scheme 2.
Proposed Reaction Cycle and Peroxide Shunt of RDD Enzymes

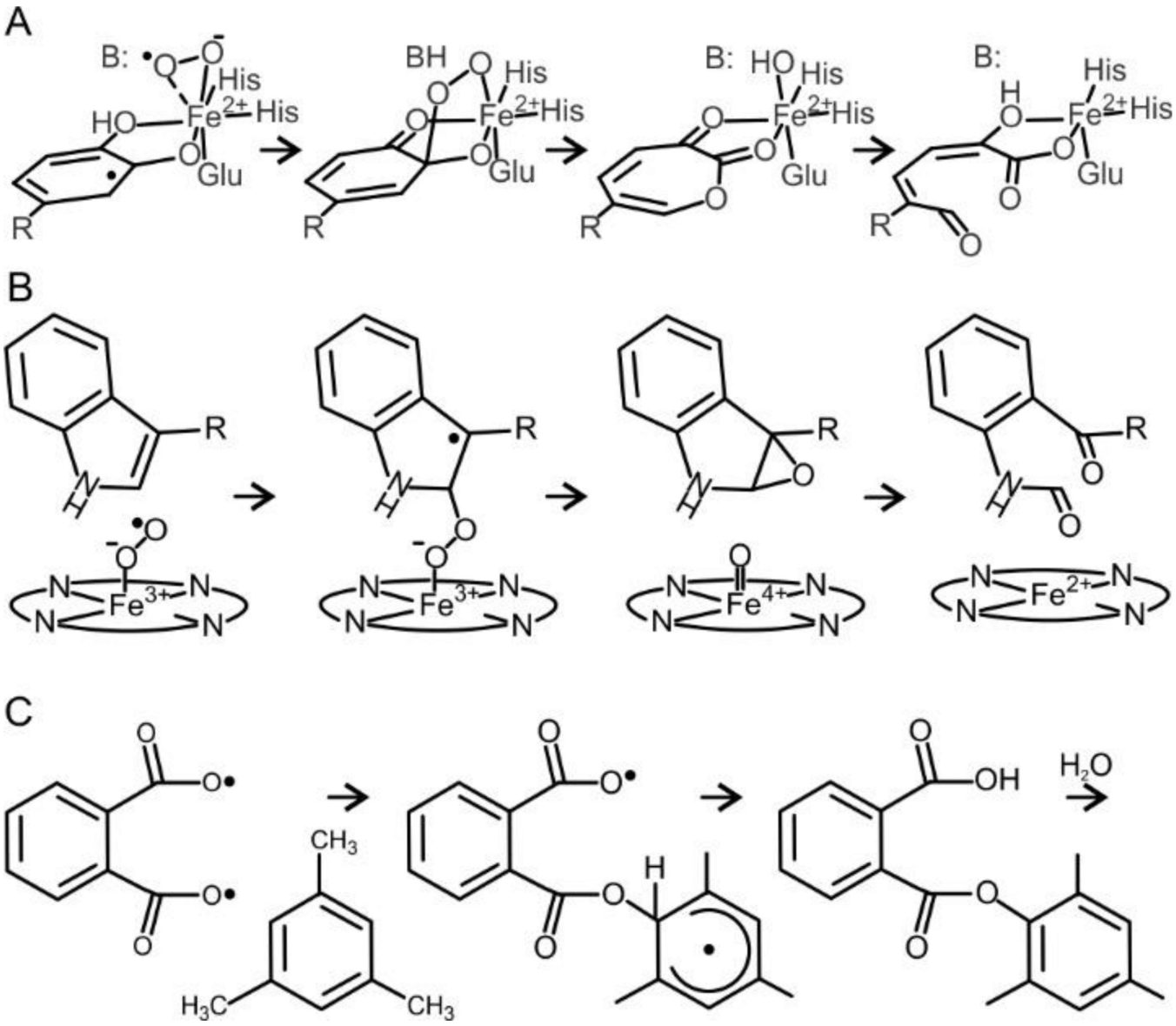

Scheme 3.

Key Steps in Reactions Mechanisms Invoking Reactive Iron-Superoxide Intermediates[a]

[a](A)Extradiol dioxygenase,[73] (B) Tryptophan 2,3-dioxygenase,[76–78] (C) phthaloyl peroxide reaction with unactivated aromatic compound.[79]

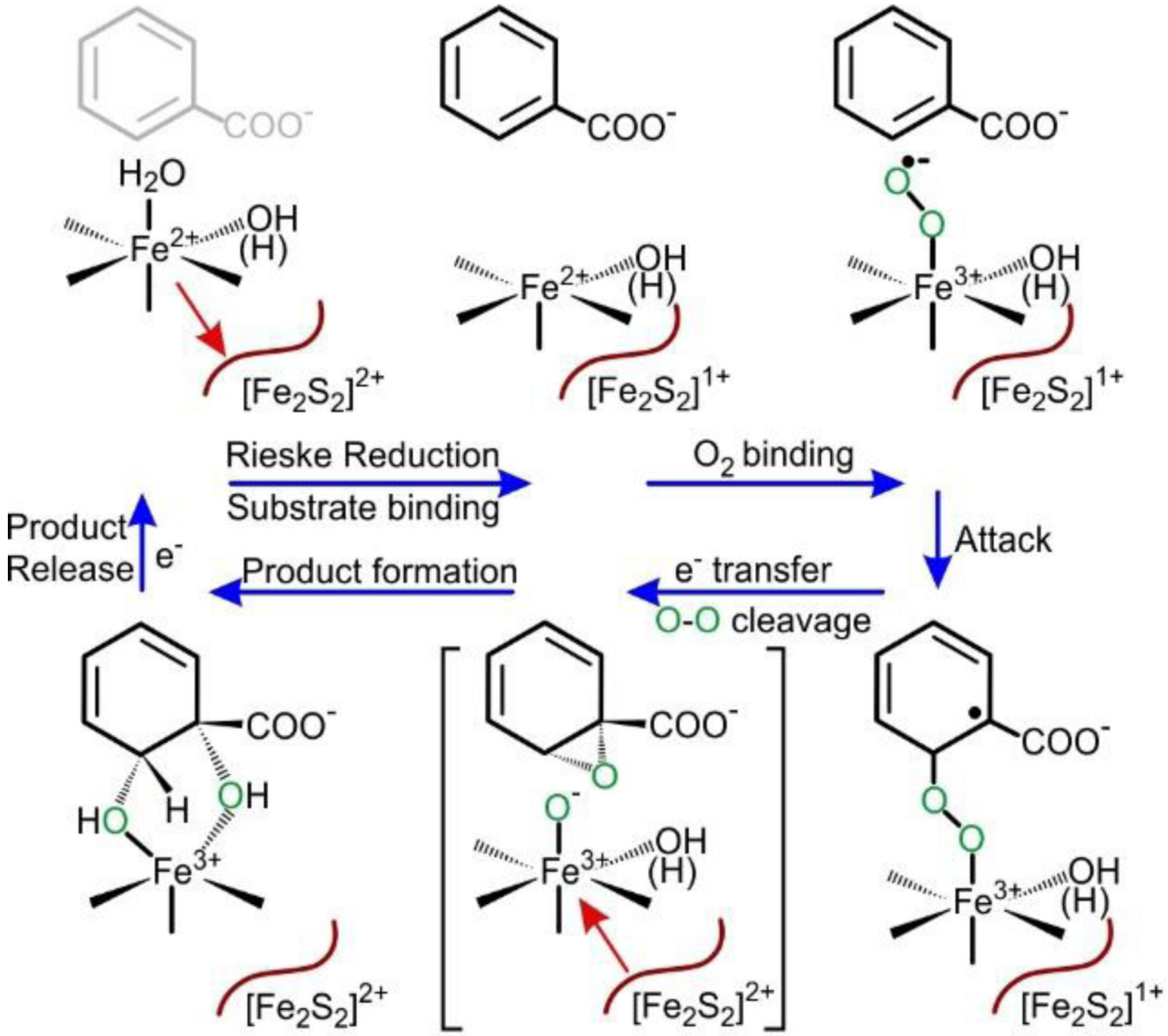

Scheme 4.

Reaction Cycle for Benzoate 1,2-Dioxygenase Emerging from the Current Studya,b,c

[a]Red arrows represent the direction of a conformational shift of the mononuclear iron observed spectroscopically and in crystal structures.

[b]There are several possibilities for the *cis*-diol forming reactions following electron transfer from the Rieske cluster, only one of which is shown.

[c]An electron from an external source is required to allow product release.

Table 1

Reaction kinetics and product formation during BZDO single turnover.[a]

	Steady State	Single Turnover									
Substrate	**O_2 uptake**	**Product formation**		**Rieske re-oxidation (464 nm)**							
				substrate coupled product forming oxidation			**substrate coupled nonproduct forming oxidation**				**Slow oxidation phases[b]**
	pK_a	**k_{cat} (s^{-1})**	**k_{obs} (s^{-1})**	**Fractional Product Yield (%)**	**RRT-1 (s^{-1})**	**% Amp**	**RRT-2 (s^{-1})**	**% Amp**	**RRT-3 (s^{-1})**	**% Amp**	**% Amp**
benzoate	4.2	4.4 ± 0.50	190 ± 50	47 ± 3	184 ± 23	49 ± 5	28 ± 3	32 ± 4	6.8 ± 1.0	14 ± 2	6 ± 2
4-fluoro-benzoate (4-FB)	4.14	0.48 ± 0.06	5.2 ± 1.2	62 ± 5	5.3 ± 0.2	70 ± 3	1.3 ± 0.3	19 ± 2			11 ± 2
3,5-difluoro-benzoate (3,5-FB)	3.5	1.0 ± 0.09	14.6 ± 0.6	63 ± 7	13 ± 1	66 ± 5	3.8 ± 0.6	22 ± 4			12 ± 2
3,4,5-trifluoro-benzoate (3,4,5-FB)	3.46	0.079 ± 0.01	0.70 ± 0.12	51 ± 8	0.86 ± 0.08	66 ± 4	0.28 ± 0.04	24 ± 3			10 ± 2

[a] Reduced BZDO was reacted with O_2 saturated buffer and the substrates shown. The steady state k_{cat}, product formation rate constant k_{obs}, fractional yield of *cis*-diol product, and RRTs and amplitudes from a multiexponential fit of the time course monitored at 464 nm were determined under the experimental conditions described in Experimental Procedures.

[b] Two low-amplitude phases much slower than the k_{cat} were observed in most cases. The slowest phase has the same RRT as the substrate free reaction (0.1 s^{-1}).

A slightly faster phase is observed only when a substrate is present, but exhibits no substrate concentration dependence.

Table 2

Kinetic parameters from substrate and O_2 concentration dependence of product coupled phase RRT-1[a]

	$K_{d,substrate}$ (μM)	$k_{forward}$ (s^{-1})	$K_{d,O2}$ (μM)	$k_{forward}$ (s^{-1})
Benzoate	191 ± 10	213 ± 4	135 ± 13	212 ± 6
4-FB	226 ± 40	5.6 ± 0.2	163 ± 12	6.4 ± 0.1
3,5-FB	950 ± 140	17 ± 1	150 ± 14	15 ± 0.4
3,4,5-FB	1800 ± 200	1.1 ± 0.1	152 ± 7	0.89 ± 0.02

[a] Apparent K_d values determined from hyperbolic fits to the data shown in Figures 4 and S2. The value for $k_{reverse}$ is approximately zero in all cases.